CHALMERS
UNIVERSITY OF TECHNOLOGY

Detection of Damage in the Equine Hoof

A possible new application for the Hot Disk Method?

Master's thesis in Engineering Physics

JENNIE SKÖLD

Department of Physics
Division of Condensed Matter Physics
CHALMERS UNIVERSITY OF TECHNOLOGY
Gothenburg, Sweden 2017

Master's thesis 2017

Detection of Damage in the Equine Hoof

A possible new application for the Hot Disk Method?

Jennie Sköld

Department of Physics
Division of Condensed Matter Physics
Chalmers University of Technology
Gothenburg, Sweden 2017

Detection of Damage in the Equine Hoof
A possible new application for the Hot Disk Method?
JENNIE SKÖLD

Supervisor: Besira M. Mihiretie, Chalmers University of Technology
Examiner: Magnus Karlsteen, Chalmers University of Technology

Master's Thesis 2017
Department of Physics
Chalmers University of Technology
SE-412 96 Göteborg
Sweden
Telephone + 46 (0)31-772 1000

Cover: Horse hooves, photo by Jennie Sköld

Printed by: Chalmers Reproservice, Gothenburg, Sweden 2017

Detection of Damage in the Equine Hoof
A possible new application for the Hot Disk Method?
JENNIE SKÖLD
Department of Physics
Chalmers University of Technology

Abstract

The detection of damages inside the equine hoof capsule, such as keratomas, cracks and infections is sometimes hard with the methods available today. A non-invasive technique that aids in the search for these conditions would be of great help in order to find these conditions without causing unnecessary damage to the horse. This study investigates a possible application for an already existing thermal transport measurement technique known as the Hot Disk Method. In this technique, a spiral shaped sensor is pressed against the surface of the material while heated by an electrical current. By measuring the resulting temperature change in the sensor, information on the underlying material's thermal properties can be obtained. The method is quick, compact and non-invasive since the total temperature increase is limited to a maximum of 5 K. Furthermore, the technique has shown capability of detecting structural changes within a material by probing the variation of thermal conductivity perpendicular to the sensor surface. Previously, tests have been conducted on conserved horse hooves where the layered structure of the hoof is detectable.

This study focuses on gathering data from live, healthy horses without any known hoof conditions in order to start building up a database of information. It is a crucial step towards the development of a possible new tool which could become an aid in the work of veterinarians and farriers in the future. Short tests to obtain information about the thermal properties of the hooves are conducted, as well as longer tests to probe the conductivity variation to see whether structural difference is also detectable in live horse hooves. Furthermore, some short measurements are conducted on conserved hooves in a controlled laboratory environment for comparison. In addition, a COMSOL model of a horse hoof is constructed, with a heat source corresponding to the Hot Disk sensor, for numerical simulation of the conductivity vs. probing depth measurements.

Keywords: equine, horse, hoof, damage, Hot Disk, thermal conductivity, COMSOL

Acknowledgements

There are so many people that have helped making this thesis possible, and for that I am very grateful. First of all, I would like to thank my supervisor Besira for all hours spent together with me during this project. Thank you furthermore for your valuable inputs and your never ending patience (and your excellent coffee cup carrying skills). Magnus, this thesis would never have happened without you. Thank you so much for giving me this chance to finish my degree in the most interesting way possible. Björn, you are an excellent farrier with an open mind. Thank you for all our interesting conversations, hopefully there will be more of those in the future. It has been great working with you! I would also like to thank the whole Transhoof project group for letting me take part in this journey. Daniel, Åsa, Arne, Maria and all the rest, you are a great group! Furthermore, a special thank you goes to the mounted police force of Gothenburg, you have been very patient with us during these past months, always cheerful and never complaining. And of course, many thanks to the fantastic police horses, it has been a pleasure working with you! I would also like to thank all my family and friends (especially Leif, who fund out and told me about this possible thesis project in the first place), for you support, you are great! Last, but definitely not least, the biggest thank you goes to my wonderful partner and friend Jonatan. You have supported me throughout these past five months in every way imaginable. THANK YOU!

Contents

1

Introduction

1.1 Background

Equestrian sports is a field which is traditionally associated with biological and veterinary research. But in the last few years, Chalmers University of Technology in collaboration with the University of Gothenburg have started an initiative in equestrian research, involving a more technological approach. The motivation is to work on behalf of the horses welfare. Horses are unable to speak, so therefore, developing non-invasive, low-stress imposing measuring methods, instruments and materials can aid our understanding of how the horses are affected by factors such as rider and equipment. The technological approach has proven to be a largely missed aspect of the equestrian world; the initiative has been of huge interest amongst riders, farriers, veterinarians and trade, to name a few [1].

An absolutely crucial part of the horse's ability to perform as an athlete is attributed to its hoof health. There is a common saying that goes "no hoof, no horse", which is just as true as it can be. Unfortunately, hoof wall damage such as hoof wall separations and cracks are common. Another hoof condition which is not quite as common but harmful non the less, is caused by abnormal keratin masses produced by epidermal cells located in the coronary band, known as keratoma [2]. These damages are believed to be caused by improper diet, environmental factors, possible inherent structural anomalies and sometimes physical endeavor, and can be of anything from minor aesthetic nature to causing complete lameness [3, 4]. The internal structures of the hoof are shown in figure 1.1.

It is sometimes hard to detect and localize damage to the hoof capsule and the underlying soft tissue, or lamina, between the hoof wall and the coffin bone using common methods such as x-ray screening and ultrasound [5]. An option would be an MRI- or CT-scan, but these techniques require highly advanced equipment which is not readily available for horses at a justifiable cost. Hence, as of yet, there is no simple, efficient and non-invasive technique to accurately localize these hoof conditions. The search for a convenient method which will potentially be used as a complement to farriers and veterinarians in the long run is therefore the scope of one of the ongoing horse related projects at Chalmers University. In collaboration with Gothenburg University and Vinnova, the project's goal is to investigate whether an already existing technique for determining the thermal transport properties of solids, powders and liquids known as the *Hot Disk Method* can be used for such an application. This study is part of that project, where the aim is to collect data from live horses without known hoof conditions to gain knowledge of what to expect from a healthy hoof.

The general principle of the Hot Disk Method was born in 1979, when a new method for measuring thermal transport properties of solids was developed by Gustavsson et. al. The technique used a thin strip-shaped metal foil piece, which was sandwiched between two specimen halves and heated by an electrical current. This heat source simultaneously served as a temperature sensor, where the temperature dependent resistance changes were monitored. From there, the temperature change in the strip could be precisely deduced and both the *thermal diffusivity* (κ) and *thermal conductivity* (λ) of the material could be determined [6, 7, 8]. This technique is referred to as the *Transient Hot Strip (THS)* technique, since it falls into one of the two broad groups into which experimental thermal conductivity measuring is normally divided, namely a *transient* technique. It is characterized by fast measurements performed on relatively small sample geometries, while the second group is known as the *steady state* techniques, which require long measurement time as well as large sample dimensions [9].

The mathematical analysis for the temperature change in the hot strip sensor is relatively

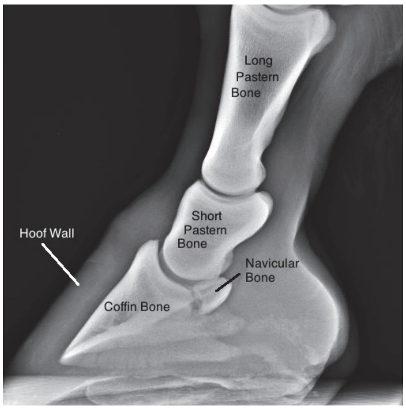

(a)

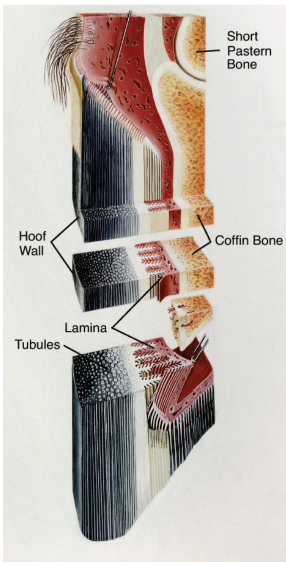

(b)

Figure 1.1: **(a)** X-ray of horse hoof. **(b)** Cross section of horse hoof, courtesy of C. Pollitt and J. McDougall, *Equine vet. Educ.* (1998) **10** (6) 318-325.

simple, providing analytical solutions. Although, the downside is that it still requires rather large sample geometries to provide reliable results. This problem was adressed by Silas E. Gustavsson at Chalmers University of Technology, Gothenburg in the early 1990's, where he solved the issue by coiling the wire into a spiral. As a result, the length of the wire (or strip) provided a much higher resistance than the hot strip sensor, resulting in higher accuracy and sensitivity. Furthermore, due to the sensor geometry, the materials studied could be much smaller than those required for the hot strip measurements. This updated version of the hot strip method is generally known as the *Transient Plane Source (TPS)* technique, or the *Hot Disk Method*. The TPS technique has many advantages; it covers a large range of thermal transport properties, it is applicable to a large number of different materials, and it is very compact [6, 8].

The heating element in the Hot Disk technique was developed from a 10 μm thin Ni strip, arranged in a spiral fashion, wedged between two 25 μm thin insulating Kapton [1] layers. The result was a very robust, easy to handle 20 mm diameter sensor with a 4 Ω resistance [10]. In addition, the electrically insulating layer provided the advantage of performing measurements on conducting samples such as metals [7]. Nowadays, the sensors come in a range of sizes depending on the type of materials and geometries to be examined. There are also three different insulating layer materials to choose from depending on the temperature range and other conditions in which the measurements are to be performed [11]. Typical Hot Disk sensors are seen in figure 1.2.

Recently, a new application to the Hot Disk method has emerged in which thermal conductivity inhomogeneities in a material can be detected. One indicator of an inhomogeneous material is obtaining different values for the thermal conductivity depending on the lateral position of the probe. Another is to identify layers of different thermal conductivity perpendicular to the sensor surface, that is, axially into the material [12]. The latter approach yields the thermal conductivity as a function of probing depth. The deviations from the curves of a homogeneous material provides information about the conductivity variations

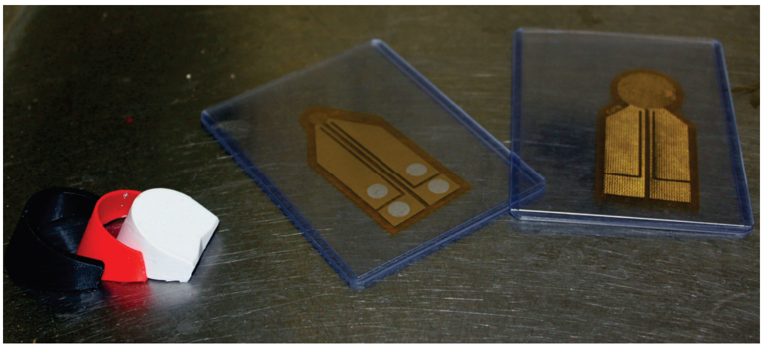

Figure 1.2: Hot Disk sensors together with 3D-printed model of the layered structure of the hoof. Photo: Mia Halleröd Palmgren/Chalmers.

[1]High performance polyimide film developed in the late 1960's by DuPont [13].

along the probing axis [9].

The equine hoof is an example of a layered structure, as seen in figures 1.1 and 1.2. If the Hot Disk method could be used to gain information about these layers that cannot be seen by the already mentioned diagnostic equipment available today, it could be of great help for the equine health professionals. There is a possibility that the conductivity vs. depth curves show significantly different behavior when applied to a damaged hoof compared with a healthy one. In this study, there are two operating modes of the Hot Disk Method used. One of them is the already described conductivity v.s probing depth, or *structural probe* mode, in which a larger sensor and relatively long measurement times are used to reach the desired probing depths. The other mode, the *isotropic*, consists of short, shallow measurements carried out with a smaller sensor. The isotropic measurements can be used to measure the thermal properties of the hoof capsule, which in turn could possibly provide information about the general health status of the hoof.

1.2 Problem Statement and Aim

Previous studies on conserved horse hooves using the Hot Disk Technique have revealed the possibility to detect the structural differences of the hoof in terms of conductivity versus probing depth. In this study, the aim is to gather data from healthy, live horses as a next step in this completely new application for the Hot Disk Method. It is a crucial step in investigating whether the method could be used to detect anomalies in the hoof capsule in the future.

The main difference when measuring on live horses compared to conserved or dried hooves is that live horses have body heat and blood circulation. In addition, horses constantly shift their weight between their different feet and they also tend to step around occasionally. These factors will cause disturbances in the measurements, especially since the equipment is very sensitive to motion and temperature change. The main problem is to find out whether key features of the hoof capsule will still be visible through the noisy data. It is also investigated if it would be possible to smooth out the data in order to reduce noise, without losing information simultaneously. Furthermore, the thermal properties of the hoof wall will be measured using short, shallow measurements.

Another aim of this study is to develop a 3D numerical model of the hoof with the sensor attached, to simulate a structural probe measurement in COMSOL multiphysics. The main idea is to find out whether it will be comparable with, and to possibly provide information about what to expect and look for in the live measurement data.

1.3 Delimitations

This study focuses on collecting data from healthy horses without any known hoof conditions in order to build a database which can be used as reference for horses with possible hoof damage in the future. Furthermore, there will be no experiments where the obtained measurement data is linked to factors associated with hoof quality and health. This is up to future study to show.

1.4 Disposition/Outline

In this thesis, the theory of heat transfer in solids will be discussed in chapter 2, along with the specific application for the Hot Disk method. A brief introduction to the COMSOL simulation software used for this work is also presented. Then, the experimental procedures are described in detail in the method section, chapter 3. The experiments have been conducted on conserved hooves in a controlled laboratory environment, as well as through field studies on live horses provided by the Gothenburg riding police department. The COMSOL simulation setup is also described in detail. In chapter 4, the results are presented along with the discussion, and finally in chapter 5 the main conclusions from this work are found.

2

Theory

In this section, the theory of heat transfer in solids will be discussed generally, as well as for the specific case of the Hot Disk Sensor. Furthermore, the idea behind the COMSOL Multiphysics software will be briefly introduced.

2.1 Heat Transfer in Solids

Transference of heat is a phenomenon that will occur when different parts of a body are at different temperatures. In order to reach thermal equilibrium, the heat will flow from the hotter parts of the body towards the cooler. This heat flow can take place in three different ways; through *conduction, convection* and *radiation*, as illustrated in figure 2.1. In the first, heat will pass through the body itself, in the second, the heat is transferred by relative motion of the body and in the third, heat is transferred by electromagnetic radiation. Convection and radiation are the central mechanisms governing the heat transfer in liquids and gases, while in solids, the first is completely absent and the second is commonly negligible. As a consequence, conduction is the dominating transport mechanism for heat transfer in solids, and it is also the phenomenon on which the theory for the method used in this thesis is based [14].

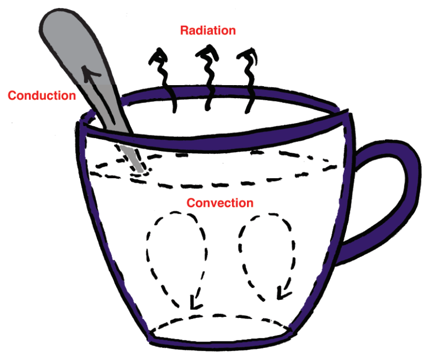

Figure 2.1: The mechanisms of heat transfer; conduction, convection and radiation.

The thermal transport properties of solid materials vary greatly depending on a number of different factors, such as structure, porosity, density and electrical conductivity to name a few. In addition, these properties can be greatly affected by temperature and pressure changes [8]. In the case of an *isotropic* material, the differential equation governing the heat transfer in the solid is given by

$$\frac{\partial^2 T}{\partial x^2} + \frac{\partial^2 T}{\partial y^2} + \frac{\partial^2 T}{\partial z^2} = \frac{1}{\kappa}\frac{\partial T}{\partial t} \rightarrow \kappa \nabla^2 T = \frac{\partial T}{\partial t}. \tag{2.1.1}$$

In (2.1.1), $\kappa = \frac{\lambda}{\rho c}$ is defined as the *thermal diffusivity* with λ, ρ and c being the *thermal conductivity, density* and the *specific heat* of the sample, respectively. $T(x, y, z, t)$ is the temperature at point (x, y, z) and time t. For small temperature changes, ρ and c are assumed to be temperature independent. The thermal conductivity λ, which is the main property of interest in this work, is a measure of a material's ability to conduct heat [6, 14].

Furthermore, if the body contains a heat source of strength Q which is switched on at $t = 0$, its' effect is included by modifying equation (2.1.1) into

$$\kappa \nabla^2 T + \frac{Q}{\rho c} = \frac{\partial T}{\partial t}, \tag{2.1.2}$$

where Q usually is a function of position and time, representing the amount of heat released at (x, y, z, t) per unit time and volume.

The general solution to (2.1.1) is well known and given by

$$T = T_0 + \frac{1}{(4\pi\kappa t)^{3/2}} \exp\left(-\frac{r^2}{4\kappa t}\right) \quad \text{for t} > 0, \tag{2.1.3}$$

with T_0 being the initial temperature and $r = (x, y, z)$. In the case of a heat source existing in the material as described in (2.1.2), the resulting general solution is a convolution of (2.1.3) and the function $\frac{Q}{\rho c}$, given by

$$T(\vec{r}, t) = T_0 + \int_0^t \int_{V'} \frac{Q(\vec{\xi}, t')}{\rho c} \frac{1}{[4\pi\kappa(t - t')]^{3/2}} \times \exp\left(-\frac{(\vec{r} - \vec{\xi})^2}{4\kappa(t - t')}\right) \mathrm{d}^3\vec{\xi}\mathrm{d}t', \tag{2.1.4}$$

where the integration is carried out over the heat source volume V' [6].

2.2 The Hot Disk Method

A heat source geometry corresponding to that of the double spiral Hot Disk sensor can be treated as m equally spaced concentric rings where a is the radius of the largest ring and a/m the radius of the smallest. The average temperature increase in the sensor surface can therefore, after some simplifications and averaging over the total length of the rings, be expressed as [6]

$$\Delta\bar{T}(\tau) = \frac{P_0}{\pi^{3/2} a\lambda} D(\tau), \tag{2.2.1}$$

where

$$P_0 = \pi a(m+1)\, Q_0 \tag{2.2.2}$$

is the output power of the sensor, and

$$D(\tau) = \frac{1}{m^2(m+1)^2} \int_0^\tau \frac{\mathrm{d}\sigma}{\sigma^2} \sum_{k=1}^{m} k \sum_{l=1}^{m} l e^{-((k^2+l^2)/m^2))/4\sigma^2} I_0\left(\frac{kl}{2m^2\sigma^2}\right). \tag{2.2.3}$$

It is clear from equation (2.2.1) that the temperature increase in the sensor is proportional to $D(\tau)$. Although this function is complicated, it can be evaluated numerically to up to six significant figures. In (2.2.3), I_0 is a first kind modified Bessel function of zeroth order described by

$$I_0\left(\frac{kl}{2m^2\sigma^2}\right) = \frac{1}{2\pi} \int_0^{2\pi} e^{\frac{kl}{2m^2\sigma^2}\sin\theta} \mathrm{d}\theta. \tag{2.2.4}$$

Furthermore, the dimensionless parameter

$$\tau = \frac{\sqrt{\kappa t}}{a} \tag{2.2.5}$$

is known as the *characteristic time ratio*, depending on the measurement time t [6]. The *characteristic time* θ of the sensor is defined as [8]

$$\theta = \frac{a^2}{\kappa}, \tag{2.2.6}$$

and the probing depth is given by

$$d_p = 2\sqrt{\kappa \times t}. \tag{2.2.7}$$

The measurement time t, or the duration of the heating current pulse, is chosen in such a way that the solid can be considered infinite. In that way, the outer boundaries of the sample will not significantly affect the temperature change in the sensor. In practice, this will require that the sample is as least as large as the diameter of the sensor. Since the measurement time should be close to the characteristic time θ, d_p is always approximately equal to the sensor diameter a [7].

The change in the sensor temperature and hence its resistance leads to voltage variations, which in turn provides precise information on the heat flow between the sensor and the test specimen. Therefore, the temperature increase in the Hot Disk sensor during a measurement can be expressed as

$$R(t) = R_0 \left[1 + \alpha \Delta T_i + \alpha \Delta \bar{T}(\tau)\right], \tag{2.2.8}$$

where R_0 is the resistance of the sensor before recording is started and α is the temperature coefficient of the resistance of the sensor material. ΔT_i expresses a small temperature drop which is caused by the thermal contact resistance of the insulating Kapton layer between the heat source and the sample material. However, the temperature drop will stabilize into a constant value after a short initialization period due to the constant power liberation [7].

The temperature development obtained from equation (2.2.8) is plotted as a function of measurement time, resulting in a graph referred to as the *transient*. A typical transient obtained from laboratory measurements on dry hoof pieces is shown in figure 2.2.

If the relationship between t, and τ is known, as it would be from equation (2.2.5) if κ were a known value, the thermal properties of the investigated material can be found by plotting the measured temperature increase $\Delta \bar{T}$ as a function of $D(\tau)$. A straight line will then be obtained, from which the thermal conductivity λ can be extracted from the slope of that line which is equal to $P_0/(\pi^{3/2} a \lambda)$, as expressed in equation (2.2.1). However, since the values for κ are generally *not* known, a series of plots are made for a range of κ values where the correct one will yield the sought for straight line. From there, the λ value can then be extracted [6].

When applying the Hot Disk technique to inhomogeneous materials, irregularities inside the material can be detected in so called *structural probing*. In such a measurement, the same experimental procedure is employed as in that of the previously mentioned case. By using an iteration scheme as presented in [12], it is possible to obtain values for the conduc-

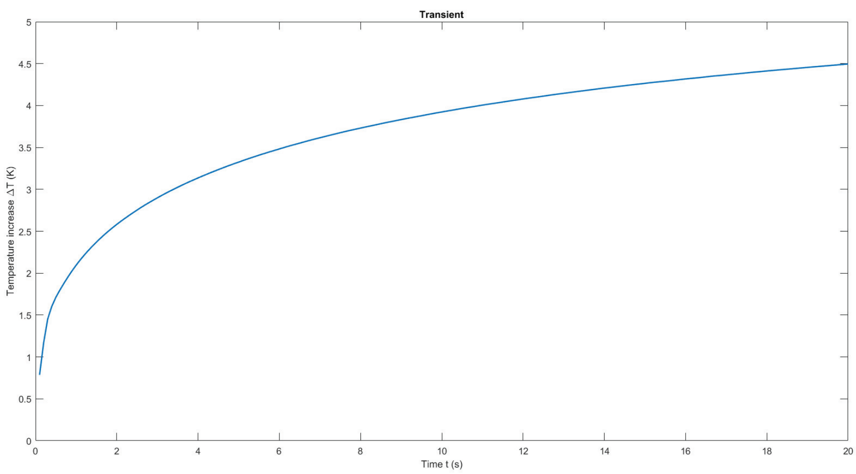

Figure 2.2: Typical transient obtained from measurements on a dried hoof piece in the laboratory.

tivity as a function of probing depth. For homogeneous materials, this method has shown to provide reproducible and accurate values. If there, for example, is a significant conductivity decrease inside the material, the value for the conductivity will drop gradually towards that of the second medium. The principle has been demonstrated experimentally on 3D-printed polymers with voids present, as illustrated in figure 2.3 [9].

Finally, when conducting experiments using the Hot Disk technique, the setup can be either one- or two sided. In a two-sided experiment, the Hot Disk sensor is wedged between two halves of the specimen. In the single-sided, the sensor is placed between the specimen and a low-conducting material such as styrofoam. Another option is to perform the measurements in vacuum The input power is adjusted in relation to the specific material and the probing time, to reach a typical total temperature increase in the sensor of 2-5 K [12].

2.3 COMSOL Multiphysics

COMSOL Multiphysics is a software platform which uses advanced numerical computation methods for simulation of physics-based problems. The program is designed in such a way that both single and coupled physics phenomena can easily be dealt with in a user friendly fashion. COMSOL has the unique feature that it automatically generates the fully coupled elements as the problem is solved. It is this patented method that is the reason why solving complex coupled multiphysics problems is possible [16].

There are a number of core physics interfaces included, such as structural analysis, electrostatics, electric currents and heat transfer to name a few. It is also possible to set up simulations by defining your own equations, with or without using the available pre-defined templates. The program also has the capability of coupling problems across spatial dimensions by, for example, being able to map a 2D solution onto a 3D-surface. Furthermore,

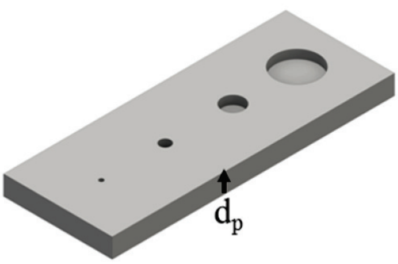

(a)

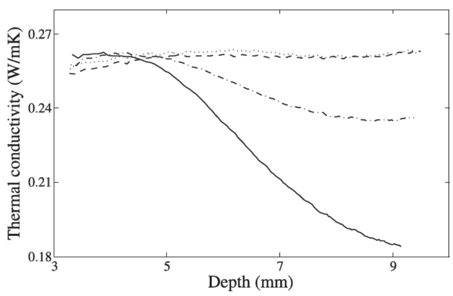

(b)

Figure 2.3: (a) 3D printed polymer slab with voids of radii 1, 2, 5 and 10 mm. (b) Conductivity vs. depth obtained from measuring along d_p in (a), using a 9.868 mm radius sensor. The solid, dash-dot, dashed and dotted lines correspond to measuring at the largest, second largest, second smallest and the smallest cavities, respectively. Courtesy of B. M. Mihiretie et. al. *AIP Advances* **6**, 085217 (2016).

problems can be solved by using several different analysis methods, but the emphasis is on the finite element method (FEM).

For this study, the heat transfer module is used where the transference of heat within, or in and out of a specific system, is studied. The module includes tools for studying all mechanisms of heat transfer, including the previously mentioned conduction, convection and radiation. Both transient and steady state simulations can be performed. Conduction, which is the main interest for this study, is the main heat transfer mechanism in solids where heat flux is considered proportional to temperature gradients in a system. This is formed mathematically by Fourier's law. Within the heat transfer module, there are a few different interfaces found, where the most interesting in the context of this study is the Heat Transfer in Solids interface. Here, the heat transfer by conduction is used as default. The other interfaces (heat transfer in fluids, porous media, bioheat and shells) also accounts for the other mechanisms by default in various combinations [15].

3

Method

In this chapter, the experimental and numerical methods employed in this thesis will be discussed.

3.1 Conserved Hooves

A typical experimental setup is shown in figure 3.1. In the laboratory, single-sided isotropic measurements were performed to find the thermal conductivity and diffusivity for a conserved hoof piece, before and after being soaked in water for several hours. Generally, the thermal properties of materials are influenced by the amount of water contained in the system. Therefore, soaking the dried hoof piece was essential to study the effects of hydration level in the sample piece. This should result in thermal properties closer to those of a live horse hoof since they naturally contain a certain degree of moisture.

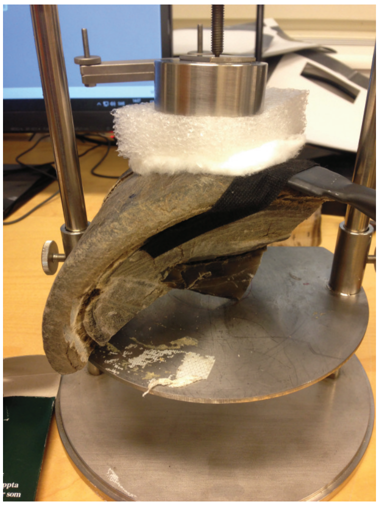

Figure 3.1: Typical experimental setup in the laboratory.

The equipment used for this work consisted of:

- Hot Disk TPS 2500 S instrument.
- Laptop with Hot Disk Thermal Constants Analyser 7.2.8 software.
- Hot Disk 7577 (2 mm radius) Kapton sensor.
- PT100 temperature sensor.
- Insulating styrofoam and cotton.
- Adjustable mounting table.
- Metal weight.

The experimental procedure begins by placing the sample on the adjustable table. The 7577 Hot Disk sensor was placed on top, in a such a way that the distance to the sample edges was large enough with respect to the sensor diameter (4 mm). Cotton and styrofoam were then placed on top of the sensor for insulation. Finally, the metal weight was placed between the styrofoam and the pressure adjusting screw at the top of the table, to put pressure on the sensor in order to create good contact with the sample. The PT100 temperature sensor was placed on the table next to the hoof piece. A number of tests were run to find the optimum input power and time settings, in order to achieve the desired temperature increase of 2-5 K. Then, three measurement sets were run. Two at an input power of 15 mW, for 10 and 20 seconds. The third set was run at 10 mW input power for 10 s.

The same procedure was employed to the soaked hoof piece. The tests before the actual measurements started revealed different optimum settings due to the altered properties of the hoof piece after soaking. Two sets of measurements were run at 10 mW input power for 20 s, and 10 mW for 40 s.

3.2 Live Horse Measurements

In addition to controlled measurements in the lab, measurements on live horses have been performed. For these measurements, 15 police horses from the Gothenburg police department were available at our disposal. The measurements were performed in the police stables during working hours. The horses were chosen for measurements in terms of availability (when off duty) and tolerance towards the equipment. Most of the horses cooperated really well, but some of them were sceptical towards the the machine and cables. Therefore, to avoid unnecessary stress for those horses and risk damage to the equipment, these horses were not measured.

Since the measurements were performed without sedating the horses, only one set of measurements on one hoof per horse was done at a time, to avoid the horses becoming too restless. One set consists of three 160 s structural probe and three 5 s isotropic measurements. In addition, a 40 s drift recording preceded each measurement. The whole procedure of attaching the sensors and cables to the horse and running the measurements, took approximately one hour. All measurements presented in this study were performed on the right fore hoof on all the horses to keep the measurements as consistent as possible, and to enable comparison on the same hoof between different occasions for those of the horses who were measured more than once.

The PT100 temperature sensor is replaced with an indoor/outdoor thermometer for the live measurements. The main reason being that at the time of measurements, the only cable available was too short to reach the horse and still allow for some movement. In addition, no extension cable was available. This would not have been a problem for measuring on sedated horses which would have been standing very still. Furthermore, the current software does not provide the ability to monitor the temperature change in the hoof, which is an important feature since the temperature in the hooves can suddenly start increasing rapidly. For the live experiments, the following equipment was used:

- Hot Disk TPS 2500 S instrument.
- Laptop with Hot Disk Thermal Constants Analyser 7.2.8 software.
- Hot Disk 8563 (9.9 mm radius) Kapton sensor with standard 50°C cable.
- Hot Disk 7577 (2 mm radius) Kapton sensor with silicone 180°C cable and LEMO-to-LEMO-FP adapter cable.
- Two 2 m long LEMO-to-LEMO extension cables.
- Indoor/outdoor thermometer.
- Wet-wrap self-adhering bandage, styrofoam and gaffa tape.
- Farrier rasp, knife, elastic rug girth, paper tissue, brush and HorslyxŮ horse-candy.

The experimental setup was assembled as follows:

1. The hoof was cleaned with brushes and paper tissue. Also, if necessary, the hoof wall was slightly polished with the farrier rasp at the chosen sensor placement location to create a smooth surface to facilitate good thermal contact.

2. To hold the cables and thermometer, an elastic rug girth was placed on the horse as illustrated in figure 3.2a.

3. Together with the temperature sensor from the thermometer, the two sensor cables were secured to the horse leg using vet-Wrap in order to reduce the risk of the horse stepping on them. This step is shown in figure 3.2b.

4. The two sensors, attached to slabs of insulating styrofoam by gaffa tape, were placed on the hoof in the desired positions. The large 8563 sensor for structural probing was placed on the center of the dorsal hoof wall, and the smaller 7577 sensor for isotropic measurements was placed on the center of the lateral side (it was hard to ensure the

exact placement since the sensors tend to move around a little in the wrapping process). The thermometer was placed somewhere convenient between the two sensors. Care was also taken to avoid placing the sensors too close to the nails attaching the horse shoes to the hoof wall, which would disturb the measurements. Finally, the sensors were firmly attached by several wraps of vet-Wrap. The final setup is shown in figure 3.2c.

With all the sensors firmly in place, a similar procedure for the measurements was carried out as for those in the laboratory. That is, the first measurements were used to find the optimum settings, resulting in an input power of 90 mW for 160 s for structural probe measurements using the larger sensor. A few structural probe measurements were also recorded at 80 mW for 320 s, to obtain a deeper probing depth. The isotropic measurements were recorded at 15 mW input power for 5 s with the smaller sensor. Furthermore, the isotropic and structural probe measurements were recorded in an alternating fashion. The reason for this was to enable the recently used sensor and hoof area to regain thermal equilibrium between measurements and still being relatively time efficient with respect to the horse.

The summary of the horses participating in this study, together with the types of measurements performed are listed in table 3.1. All horses in this study are warmblooded geldings, except from number nine, Viola, who is a shire horse mare. Furthermore, all horse's hooves were black (pigmented) except from Bentley's and Viola's, who were white (unpigmented) and black/white, respectively.

(a) (b) (c)

Figure 3.2: Experimental setup. (a) Rug girth, thermometer and cables. (b) Securing cables to the horse's leg. Photo: Mia Halleröd Palmgren/Chalmers. (c) Final assembly.

Table 3.1: Overview of the horses and types of measurements performed; Structural Probe (Sp) and Isotropic (Iso).

Horse	Sp1	Sp2	Sp3	Iso1	Iso2	Iso3
1. Bentley	1×160 s	3×160 s	-	-	3×5 s	-
2. Billy	3×160 s	3×160 s	-	2×5 s	3×5 s	-
3. Nixon	3×160 s	2×320 s	-	3×5 s	2×5 s	-
4. Pikeur	2×160 s	3×160 s	-	2×5 s	3×5 s	-
5. Robben	3×320 s	1×160 s	-	3×5 s	-	-
6. Tor	3×160 s	-	-	3×5 s	-	-
7. Urax	3×160 s	3×160 s	3×160 s	3×5 s	3×5 s	3×5 s
8. Viggo	3×160 s	3×160 s	-	3×5 s	3×5 s	-
9. Viola	3×160 s	2×160 s	-	3×5 s	3×5 s	-

3.3 COMSOL Multiphysics Simulation

For simulating heat flow in the hoof, the heat transfer in solids module in COMSOL multiphysics was used. The simulation geometry is seen in figure 3.3. Here, the outermost layer represents the hoof wall, the intermediate layer is the lamina and the inner structure is the hoof bone as shown in figure 1.1. There are some significant structural differences between figure 1.1 and the COMSOL model, but it should still give a decent simulation of the heat flow throughout the hoof capsule and into the lamina and bone regions. The Hot Disk sensor is represented by the thin concentric cylinders attached to the hoof wall.

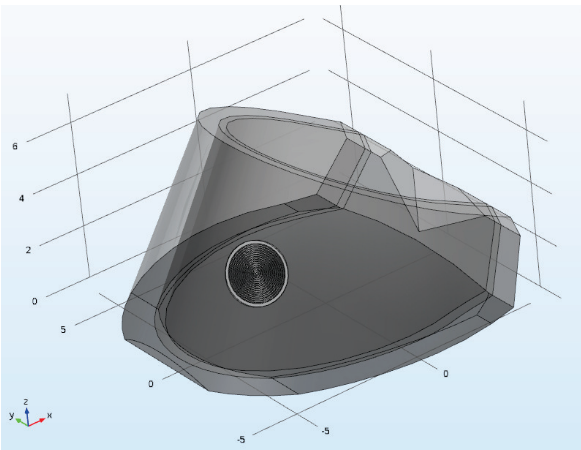

Figure 3.3: Complete geometry of hoof structure, constructed using eccentric cones, spheres, cylinders etc. The outer domain represents the hoof wall, the central domain the lamina and the inner domain the hoof bone. The sensor is constructed by concentric cylinders on the surface of the hoof wall.

In order to mimic a live horse hoof, the simulation run in two steps. First, a steady state computation without the heat source (sensor) activated is done to obtain a temperature gradient through the hoof wall. The second step is a time dependent study, where the resulting gradient from step one is used as initial conditions when the heat source is switched on for 160 s. The resulting temperature development in the sensor is then extracted from the software for data analysis through Matlab and the Hot Disk software.

The different layers of the hoof, along with initial and boundary conditions for the first step of the study is defined as follows:

1. The outermost layer, the hoof wall, consists of keratin. The outer hoof wall surface temperature was set as a fixed temperature boundary condition, according to a typical temperature measured during the experimental work, 29°C $\simeq$ 302 K. The initial temperature of this domain was also set to be 302 K.

2. The second layer represents the lamina, where the hoof's blood supply is located. Therefore it is given a slightly higher initial temperature, closer to that of the body temperature of the horse (normally around 37-38°C) at 32°C $\simeq$ 305 K. The inner boundary of the lamina, adjacent to the hoof bone, is set as a fixed temperature boundary condition of 305 K, which is the same temperature as for the domain. The reason the horse's actual body temperature isn't used is because the blood has to travel a relatively long way down to the hooves through the horses' legs which, in the lower parts, only consists of bone, tendons and ligaments [17]. Since the lamina consists of soft body tissue and blood, its properties will be approximated to those of water.

3. The innermost structure, the hoof bone, will be given the same initial temperature as the lamina, and material properties corresponding to those of bone tissue. This region will not have any boundary conditions applied.

4. The sensor is made from Nickel, and it is the source from which the heat pulse is emitted. The temperature of the sensor is set as a fixed temperature boundary condition at 302 K, and its initial domain temperature is set to the same.

For the second step of the study, the fixed temperature boundary condition on the sensor is removed to allow for it to heat up during the 160 s simulation. The material parameters used are presented in table 3.2.

The COMSOL simulation will provide the temperature change in the sensor as a function of time (and hence penetration depth) in a simulated structural probe measurement (160 s, Hot Disk 8563 sensor). In the live measurements, the Hot Disk software uses the recorded voltage differences as input data and calculate temperature change. Then, it converts the recorded transient into a conductivity versus penetration depth curve. In order to compare simulation with experimental results, the temperature increase data therefore needs to be converted into voltages before being inserted into the Hot Disk software for further analysis.

Table 3.2: Material parameters and initial values used in the COMSOL heat flow simulation.

Domain	Material	Initial Temperature [K]	Heat Capacity [J/(kg·K)]	Thermal Conductivity [W/(m·K)]	Density [kg/m^3]
Sensor	Nickel	302	445	90.7	8900
Hoof wall	Keratin	302	1800	0.4	1100
Lamina	Water	305	4178	0.59	996
Hoof bone	Bone	305	1313	0.32	1908

4

Results

4.1 Conserved Hooves

The thermal conductivities and diffusivities obtained from the isotropic measurements on dried and soaked hoof pieces are presented in tables 4.1 and 4.2, respectively. The obtained values are stable and reproducible, with conductivities ranging between 0.33 and 0.34 W/mK, and diffusivity values between 0.20 and 0.24 mm^2/s for the dry piece. After soaking, the values for the conductivity have increased to between 0.37 and 0.38 W/mK, and the diffusivity have decreased to lie between 0.11 and 0.12 mm^2/s, but remains stable and reproducible. The initial temperatures were stable to 0.1 °C throughout each measurement set. The measurements are few, and therefore, no major conclusions should be drawn at this point. Still, it gives an indication of what results to expect from conserved hoof measurements.

Table 4.1: Thermal conductivity λ (W/mK) and diffusivity κ (mm^2/s) values from isotropic measurements on dry hoof wall piece.

	15 mW, 10 s		15 mW, 20 s		10 mW, 20 s	
	λ	κ	λ	κ	λ	κ
	0.3352	0.2361	0.3373	0.2001	0.3359	0.2003
	0.3352	0.2353	0.3330	0.2022	0.3355	0.2053
	0.3355	0.2371	0.3330	0.2022	0.3358	0.2066
	0.3348	0.2361	0.3268	0.2156	-	-
Average	**0.3352**	**0.2362**	**0.3325**	**0.2050**	**0.3357**	**0.2041**
Std dev	0.00024	0.0006	0.0038	0.0061	0.0001	0.0027

Table 4.2: Thermal conductivity λ (W/mK) and diffusivity κ (mm^2/s) values from isotropic measurements on wet hoof wall piece

	10 mW, 20 s		10 mW, 40 s	
	λ	κ	λ	κ
	0.3706	0.1176	0.3738	0.1183
	0.3749	0.1314	0.3730	0.1085
	-	-	0.3818	0.1204
	-	-	0.3809	0.1172
Average	**0.3727**	**0.1245**	**0.3774**	**0.1161**
Std dev	0.0022	0.0069	0.0040	0.0045

4.2 Live Horse Measurements

Due to the reasons described earlier in the method section, there are not an equal number of measurements for all horses available, although all but one horse were measured at least twice. An advantage of having several measurements on the same horse taken at different occasions is the ability to compare the individual variations. Horse number seven, Urax, was particularly interesting since he stood very still during the first set of measurements, but was significantly more restless at the next two occasions causing more noise in the obtained transient data. This is especially reflected in the longer structural probe measurements and hence affects the conductivity vs. depth curves.

Some measurements have had to be discarded due to reasons such as bad contact between the sensor and the hoof, faulty temperature input, problems with the equipment etc.

4.2.1 Isotropic Measurements

In table 4.3, the measured conductivity and diffusivity values are given with four significant digits, together with the recorded initial temperatures before each measurement. Table 4.4 presents the averages and standard deviations for each horse. Here, the average conductivity values lie within the range of 0.36 - 0.46 W/mK, and the diffusivity lies within 0.20 - 0.51 mm^2/s.

The standard deviations varies significantly, since the recorded values are scattered over a larger range for the live hooves than for the conserved ones. This is especially true for the diffusivity measurements. Although, some of the values deviating the most from the averages could possibly be the results of disturbances (noise, sensor contact, fluctuating temperatures) during the measurements. Another reason as to why the diffusivity varies so much could be that the hoof is not actually an isotropic material. If the material is anisotropic, the isotropic measurements would not provide the correct values. Hence, for this specific application, anisotropic measuring which also an option in the Hot Disk software, could possibly have been a better option.

It is also clear that the initial temperature of the hoof can vary greatly, not only between horses, but also during one measurement on the same horse. In addition, it also varies from occasion to occasion in the same horse, as for example is seen in horse number seven, Urax. In the second set of measurements, his hoof temperature increased from 27.2°C to 29.8°C during the time of the measuring, while in the third set, it stayed nearly constant at 14°C. Furthermore, the temperature increase can commence quite suddenly. Generally this could possibly be dealt with by making sure the setup is given enough time to stabilize, monitoring the temperature increase rate, before the measurements starts. The Hot Disk software is capable of compensating for temperature drift in the 40 s drift measurement preceding the actual measurement, although if sudden temperature changes occur after the drift measurement has finished, it will affect the results. Since the isotropic measurements are short, the probability for such sudden temperature increase occurring during the measurement time is naturally lower.

Only horses number one and nine, Bentley and Viola, have unpigmented, or partially pigmented hooves. Looking at the values in table 4.3, there is no significant difference between the values obtained from the pigmented hooves. It could be possible that there is a difference, but it is not large enough to be detectable within the span of values obtained for the nine horses in this study. In addition, Viola is the only mare and furthermore the only horse of different breed, but there are no apparent differences between the values obtained from her hoof and the others. Although, this is only one horse. For reliable conclusions, more measurements are needed on larger groups of same-sex and -breed horses. Further studies on larger groups of horses with pigmented and unpigmented hooves would also be advisable before any major conclusions are drawn.

Table 4.3: Initial temperature T_i (°C), thermal conductivity λ (W/mK) and diffusivity κ (mm^2/s) values from isotropic measurements.

	Set 1 (Iso1)			Set 2 (Iso2)			Set 3 (Iso3)		
Horse	T_i	λ_1	κ_1	T_i	λ_2	κ_2	T_i	λ_3	κ_3
	27.0	0.4170	0.7015	-	-	-	-	-	-
1. Bentley	29.3	0.4042	0.3943	-	-	-	-	-	-
	30.2	0.4103	0.3970	-	-	-	-	-	-
	28.5	0.3873	0.2274	20.5	0.4100	0.4030	-	-	-
2. Billy	29.6	0.3364	0.1640	23.5	0.4156	0.4470	-	-	-
	-	-	-	24.3	0.4075	0.2909	-	-	-
	25.6	0.3972	0.2569	28.8	0.3970	0.2420	-	-	-
3. Nixon	26.2	0.4490	0.4167	32.1	0.3637	0.1956	-	-	-
	25.9	0.4292	0.7253	-	-	-	-	-	-
	24.0	0.4803	0.4852	20.0	0.4246	0.4147	-	-	-
4. Pikeur	28.0	0.4412	0.3198	23.0	0.4287	0.4168	-	-	-
	-	-	-	26.5	0.4175	0.3555	-	-	-
	11.8	0.4430	0.4296	-	-	-	-	-	-
5. Robben	11.9	0.4313	0.3769	-	-	-	-	-	-
	11.9	0.4346	0.4088	-	-	-	-	-	-
	24.0	0.4325	0.4307	-	-	-	-	-	-
6. Tor	28.1	0.4152	0.3496	-	-	-	-	-	-
	30.8	0.4353	0.4098	-	-	-	-	-	-
	18.0	0.3727	0.2178	27.2	0.3946	0.2748	14.3	0.3880	0.3628
7. Urax	19.2	0.4191	0.2968	29.2	0.3978	0.2319	13.8	0.4030	0.2776
	20.5	0.3723	0.2137	29.8	0.4105	0.2955	13.8	0.4025	0.4038
	29.0	0.4296	0.3096	11.6	0.4073	0.3631	-	-	-
8. Viggo	30.5	0.4493	0.3884	11.8	0.3952	0.2727	-	-	-
	30.9	0.4528	0.3948	11.9	0.4026	0.3015	-	-	-
	25.7	0.3566	0.2500	19.2	0.4177	0.5660	-	-	-
9. Viola	27.4	0.4354	0.4352	23.0	0.4216	0.5200	-	-	-
	28.5	0.4119	0.3635	25.5	0.4222	0.4579	-	-	-

Table 4.4: Averages (Av.) and Standard Deviation (S.d.) of thermal conductivity λ (W/mK) and diffusivity κ (mm^2/s).

Horse		Set 1 λ_1	Set 1 κ_1	Set 2 λ_2	Set 2 κ_2	Set 3 λ_3	Set 3 κ_3
1. Bentley	Av.	**0.4105**	**0.4976**	-	-	-	-
	S.d.	0.0052	0.1442	-	-	-	-
2. Billy	Av.	**0.3618**	**0.1957**	**0.4111**	**0.3803**	-	-
	S.d.	0.0254	0.0317	0.0034	0.0657	-	-
3. Nixon	Av.	**0.4251**	**0.4663**	**0.3803**	**0.2188**	-	-
	S.d.	0.0213	0.1944	0.0166	0.0232	-	-
4. Pikeur	Av.	**0.4607**	**0.4025**	**0.4236**	**0.3957**	-	-
	S.d.	0.0195	0.0827	0.0046	0.0284	-	-
5. Robben	Av.	**0.4363**	**0.4051**	-	-	-	-
	S.d.	0.0049	0.0217	-	-	-	-
6. Tor	Av.	**0.4277**	**0.3967**	-	-	-	-
	S.d.	0.0089	0.0344	-	-	-	-
7. Urax	Av.	**0.3881**	**0.2428**	**0.4010**	**0.2674**	**0.3978**	**0.3814**
	S.d.	0.0220	0.0382	0.0069	0.0265	0.0070	0.0169
8. Viggo	Av.	**0.4439**	**0.3643**	**0.4017**	**0.3125**	-	-
	S.d.	0.0102	0.0388	0.0050	0.0377	-	-
9. Viola	Av.	**0.4013**	**0.3496**	**0.4205**	**0.5146**	-	-
	S.d.	0.0331	0.0762	0.0020	0.0443	-	-

4.2.2 Structural Probe Measurements

For the structural probe measurements, the resulting transient as well as the calculated conductivity vs. depth data obtained are extracted from the Hot Disk file and plotted in Matlab.

In figures 4.2 - 4.12, the structural probe measurements are presented for the nine horses. The majority were recorded at 90 mW for 160 s, although in figures 4.5 and 4.9, data was recorded at 80 mW for 320 s to obtain a deeper probing.

The measurement is really sensitive to motion, which became very apparent in the structural probe measurements. The slightest steps from the horses are clearly visible as sudden bumps in the transients and are reflected as peaks of various sizes in the conductivity vs. depth curves. This could easily be minimized by sedating the horses during the measurements, but since they were performed at the police stables at working hours, it was not a good option in this case.

In the less noisy measurements, for example as seen in figures 4.2, 4.3, 4.4, 4.7 and 4.12 an amplitude increase is generally seen around 4-5 mm. In 4.9, the change is seen at 7-8 mm depth, however that measurement is longer and it is not known yet exactly how the different settings affect the structural probe results. Continuing deeper, the amplitude generally continues to increase.

An interesting structural feature of the hoof wall are the tubules which are seen in figure 4.1. These become larger and more spread out the further away from the surface and closer to the lamina they are located, leading to a gradient in tubule density. This, in turn, results in a water content gradient across the hoof wall [18], which could possibly be a reason for the changing behavior of the conductivity along the probing depth. One should also note, when interpreting the conductivity vs. depth data, that hoof wall thickness is individual. Furthermore, it also depends on the placement of the sensor on the hoof wall, since the hoof capsule is thicker down by the ground and very thin just below the coronet.

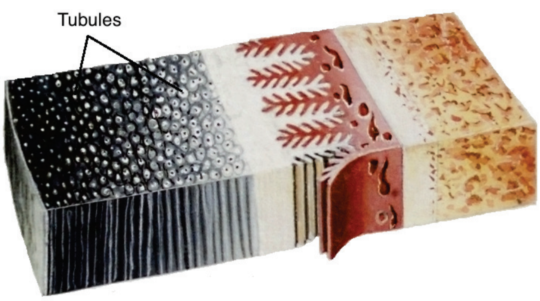

Figure 4.1: Hoof wall tubules change structure throughout the hoof wall. Courtesy of C. Pollitt and J. McDougall, *Equine vet. Educ.* (1998) **10** (6) 318-325.

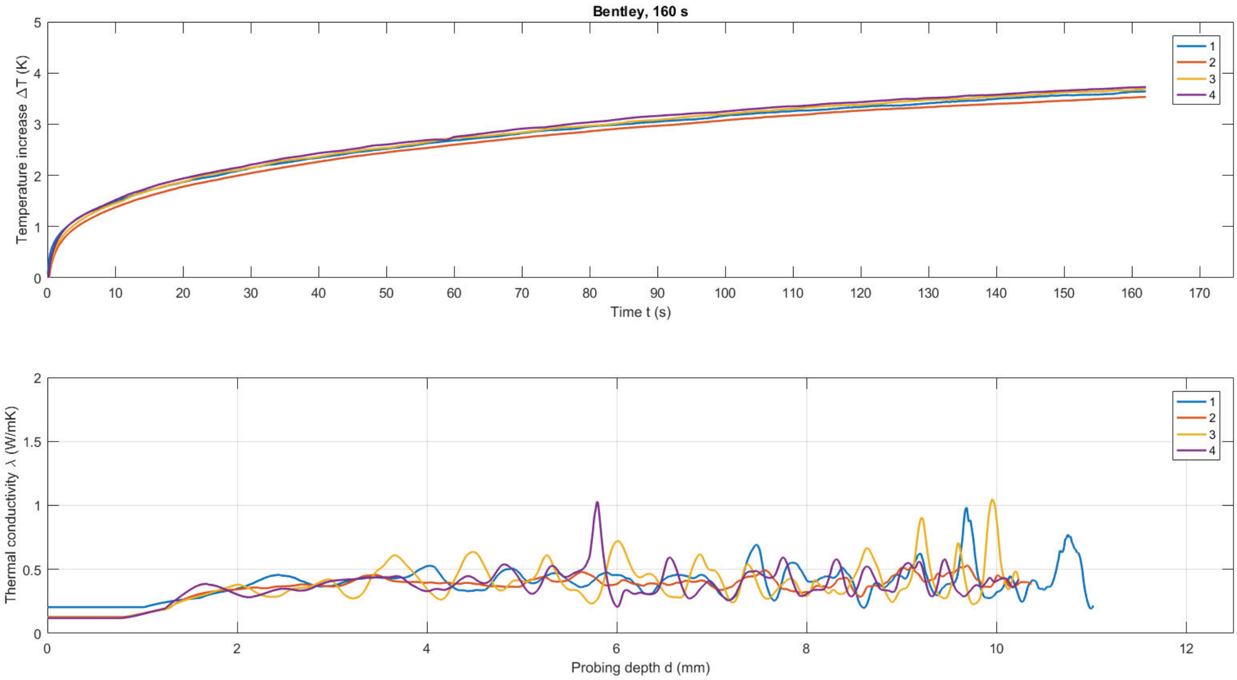

Figure 4.2: Transients and conductivity vs. depth curves obtained for Bentley at 90 mW input power for 160 s.

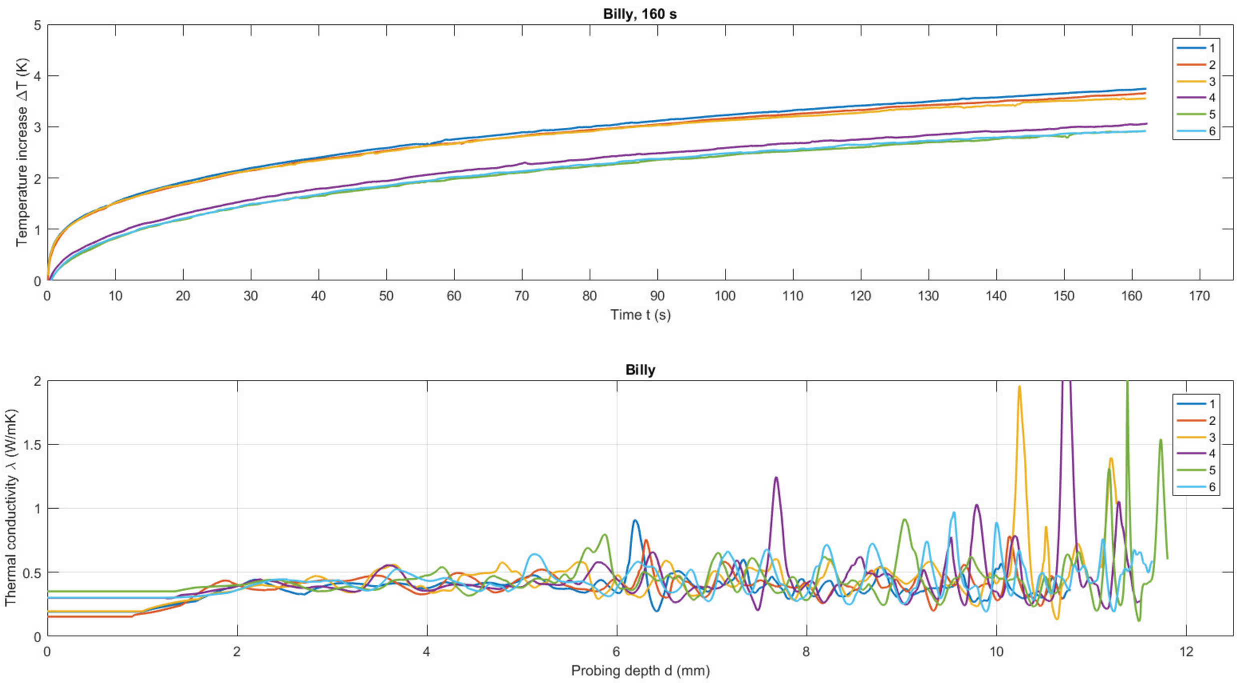

Figure 4.3: Transients and conductivity vs. depth curves obtained for Billy at 90 mW input power for 160 s.

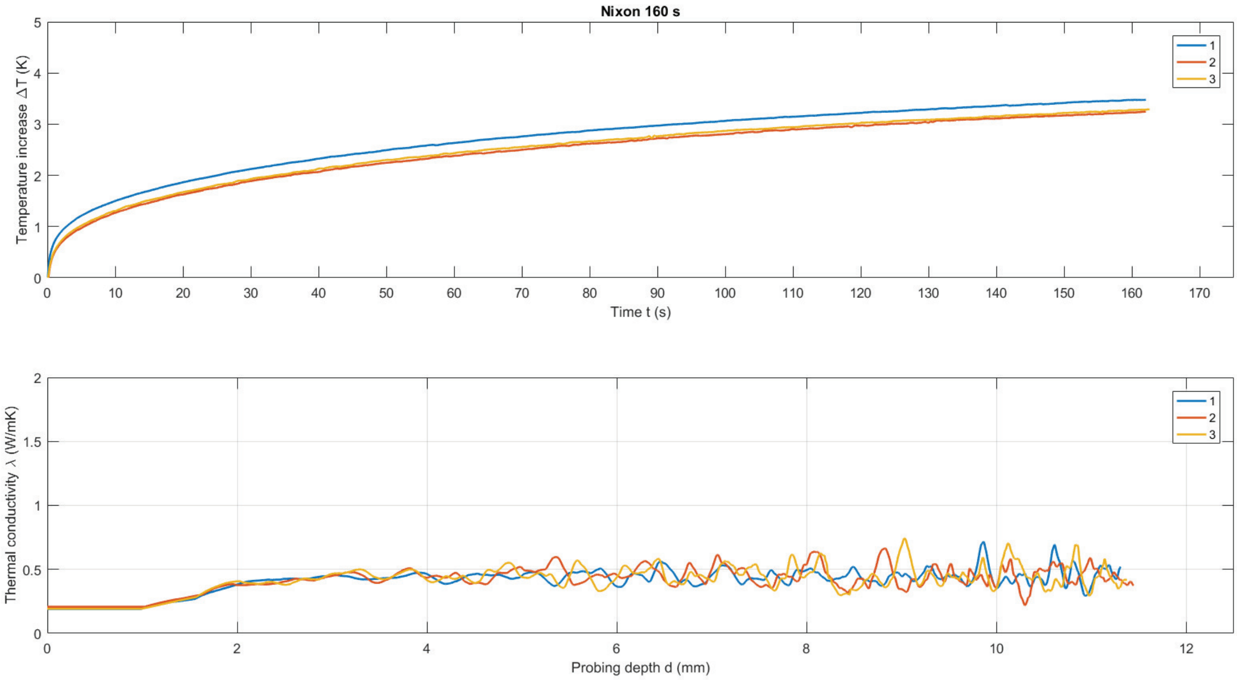

Figure 4.4: Transients and conductivity vs. depth curves obtained for Nixon at 90 mW input power for 160 s.

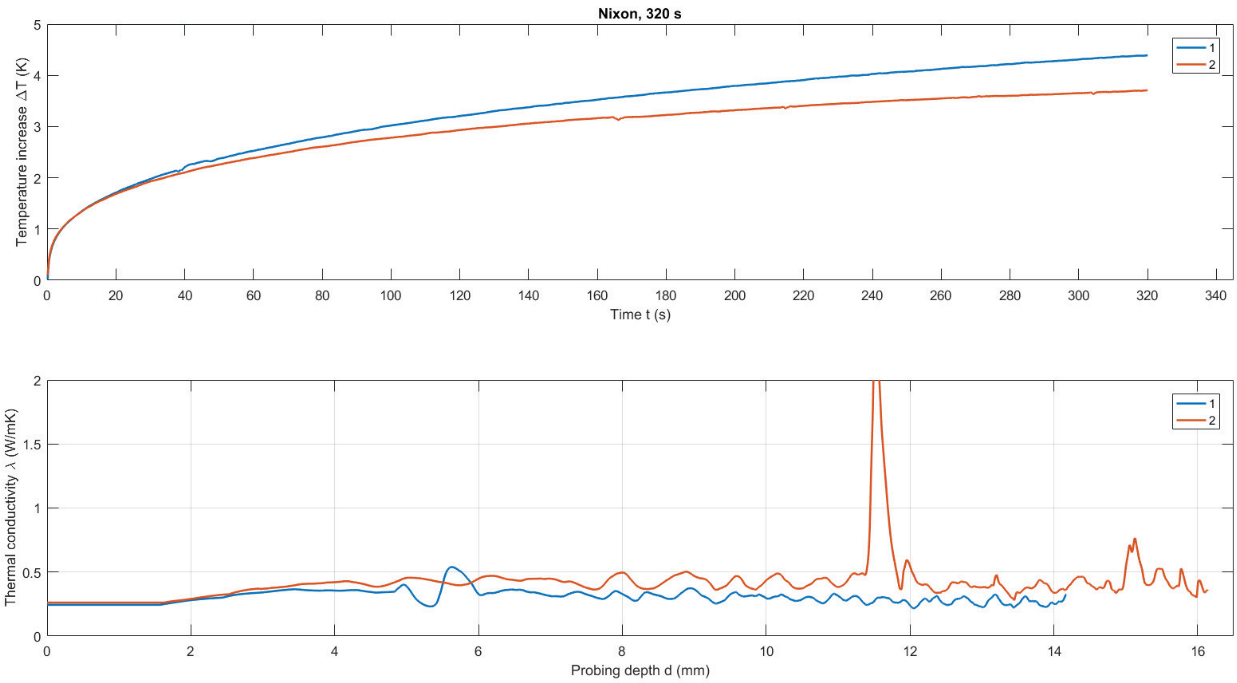

Figure 4.5: Transients and conductivity vs. depth curves obtained for Nixon at 80 mW input power for 320 s.

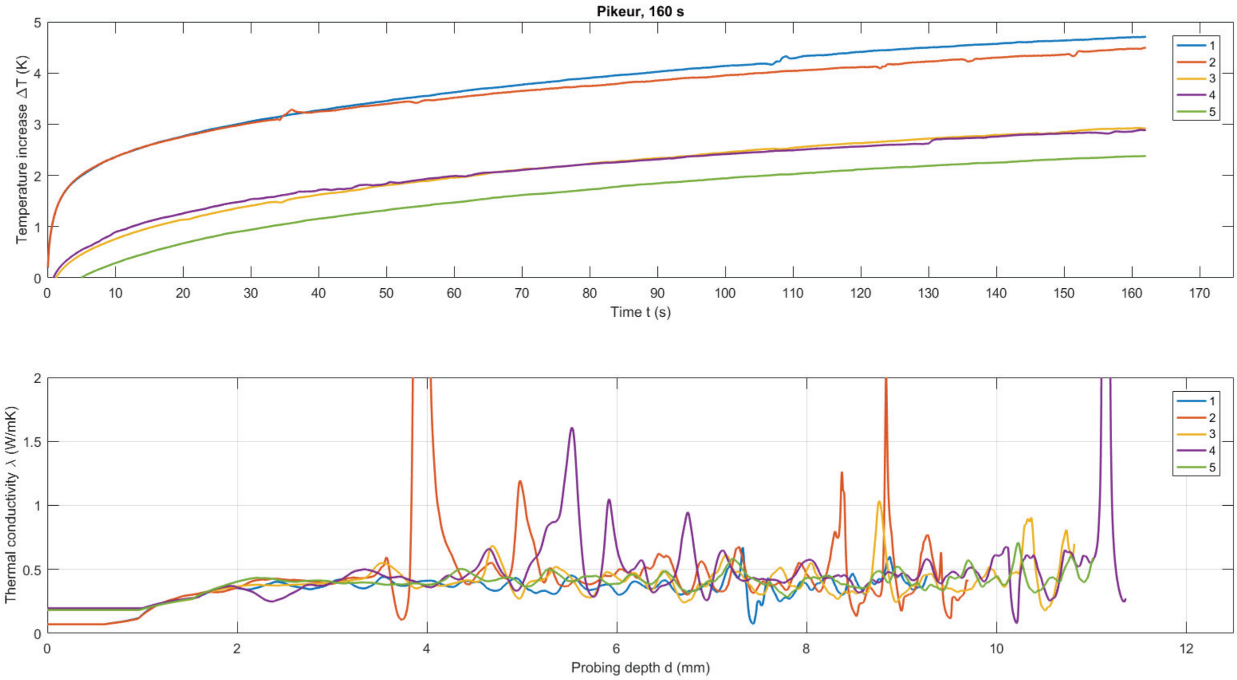

Figure 4.6: Transients and conductivity vs. depth curves obtained for Pikeur at 90 mW input power for 160 s.

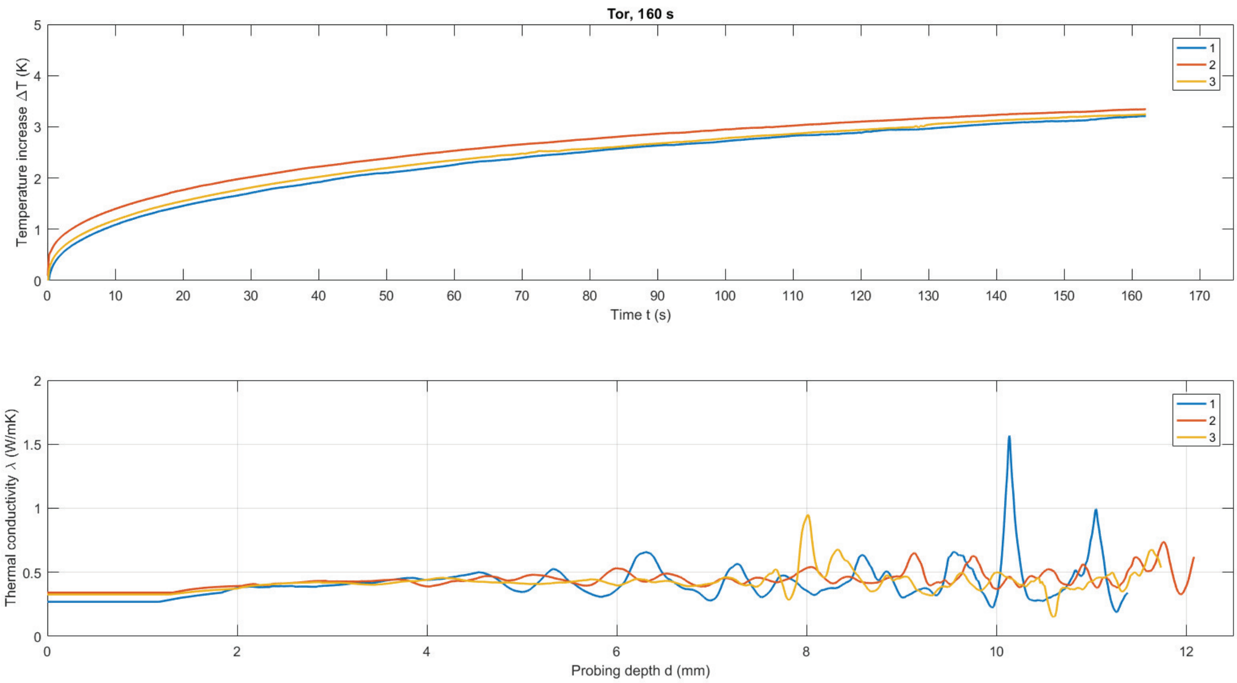

Figure 4.7: Transients and conductivity vs. depth curves obtained for Tor at 90 mW input power for 160 s.

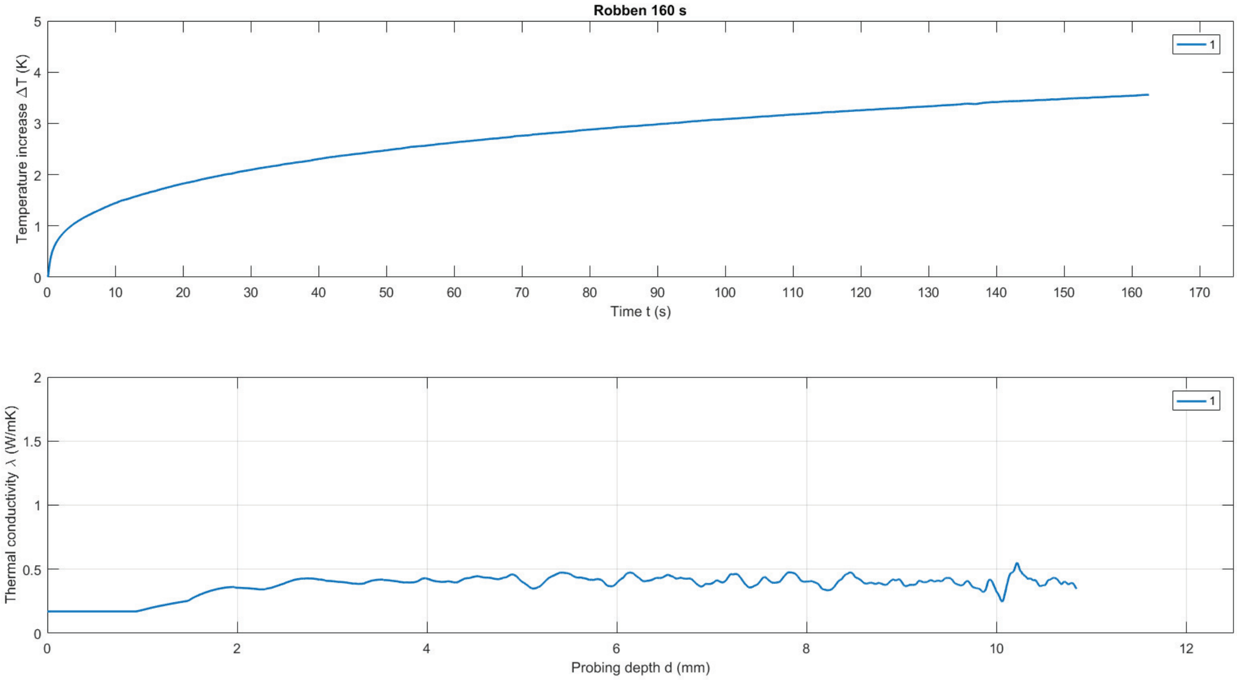

Figure 4.8: Transient and conductivity vs. depth curve obtained for Robben at 90 mW input power for 160 s.

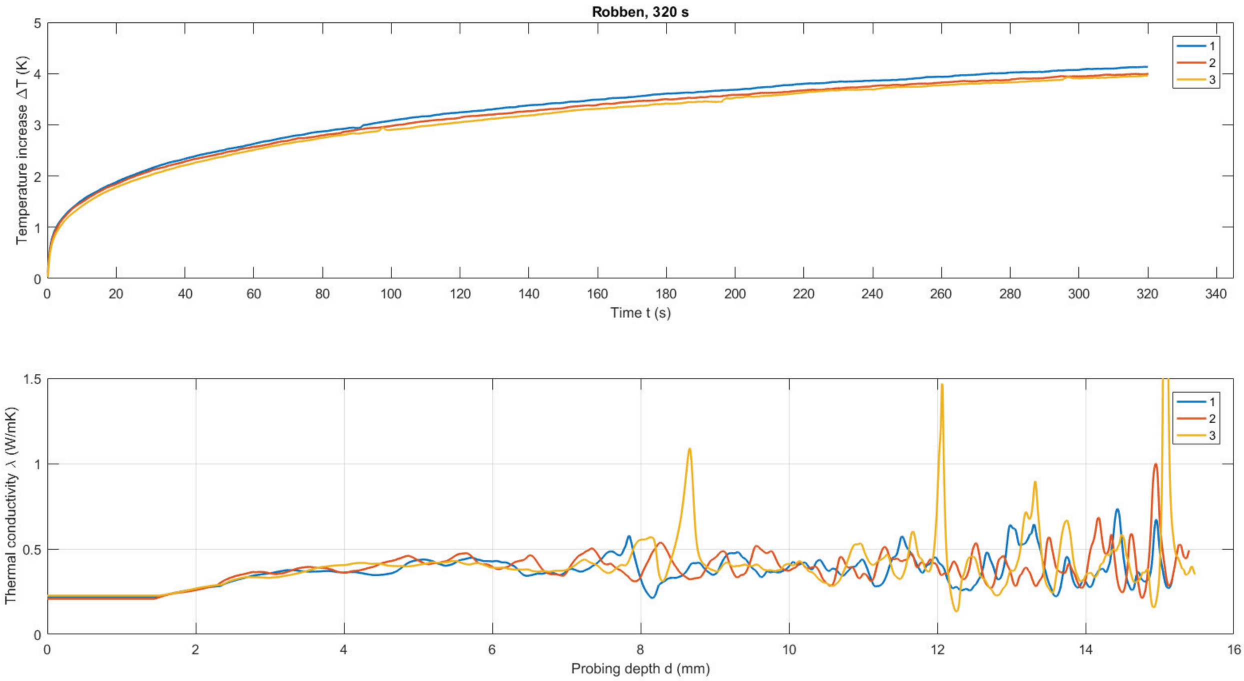

Figure 4.9: Transients and conductivity vs. depth curves obtained for Robben at 80 mW input power for 320 s.

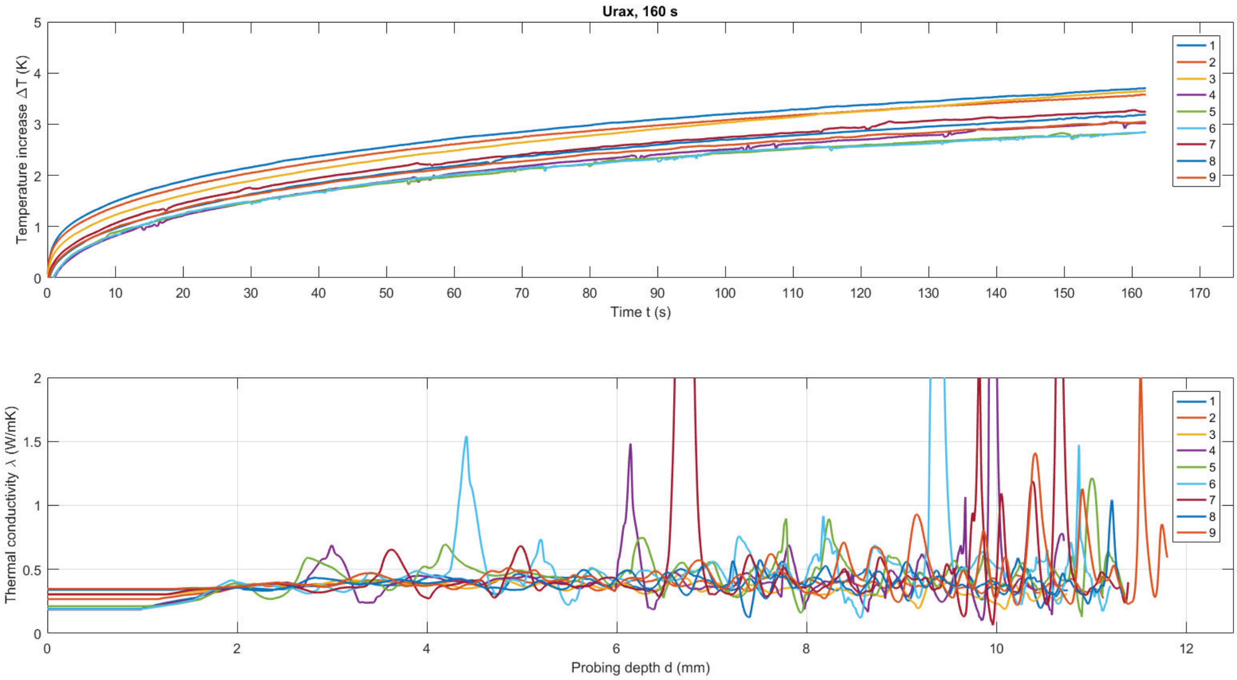

Figure 4.10: Transients and conductivity vs. depth curves obtained for Urax at 90 mW input power for 160 s.

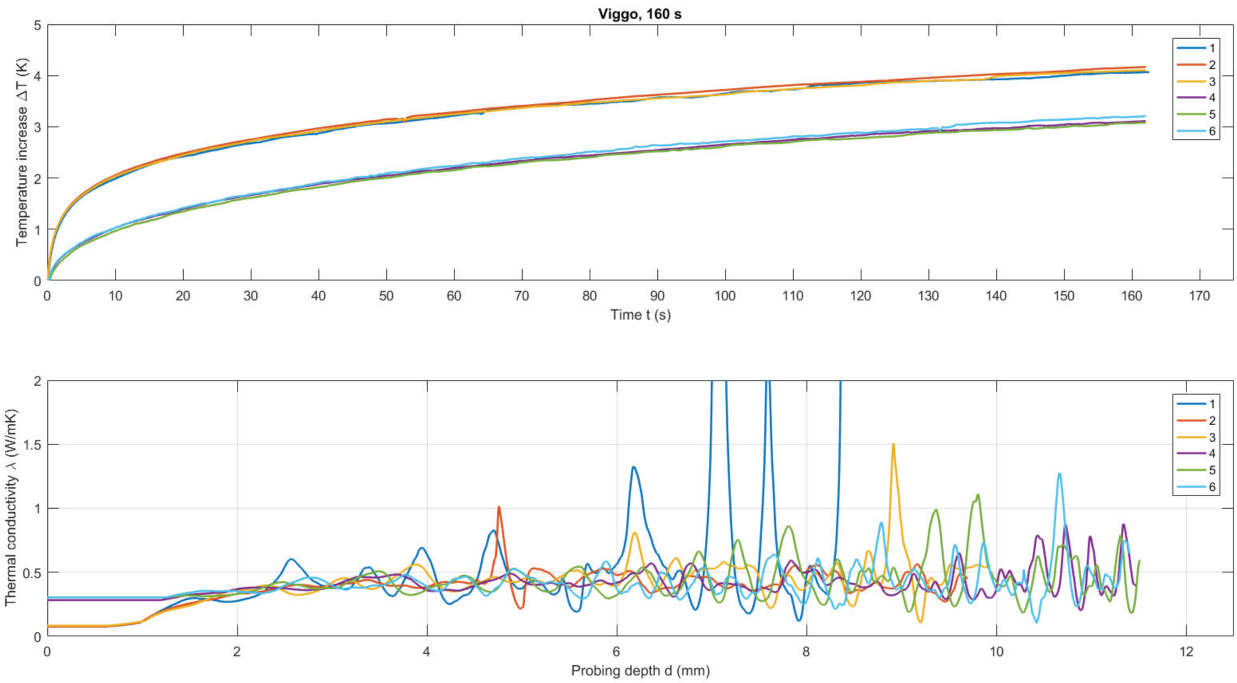

Figure 4.11: Transients and conductivity vs. depth curves obtained for Viggo at 90 mW input power for 160 s.

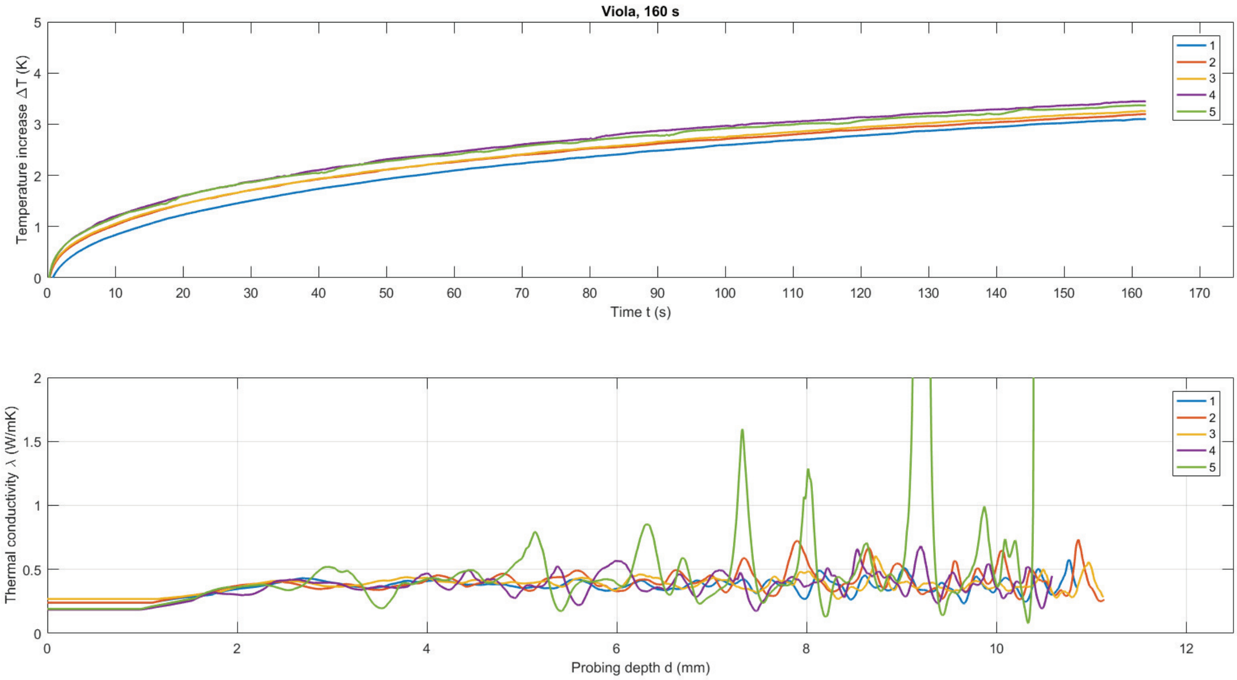

Figure 4.12: Transients and conductivity vs. depth curves obtained for Viola at 90 mW input power for 160 s.

4.2.3 Data analysis

The obtained transient data is more or less noisy for all the horses, likely due to movement and blood circulation in the hoof. Therefore, an attempt to smooth out the peaks in the original transient data is done in Matlab. The data then is re-inserted into the Hot Disk software to calculate the resulting conductivity vs. depth curves again, and compared with the original ones.

As previously mentioned, there are three sets of measurements for Urax. Since he stood very still during the first measurements and was much more restless at the following two occasions, he is a good example to try the data smoothing on. The results are shown in figure, 4.13 - 4.18. It is apparent that the conductivity versus depth data becomes much more stable after smoothing, and all major peaks have been removed.

There is a risk that important information is lost in the smoothing process. Although, it seems as if the apparent structural change at around 5-6 mm depth is still there, where the amplitude of the oscillations in the curves is increasing. It should be noted however that the smoothing function used for this purpose, causes a relatively large deviation from the original transient in the first 10-15 seconds of the transients. Therefore the resulting conductivity vs. depth values for the initial part of the curve should be ignored. It also appears to cause a shift in the probing depth in various directions.

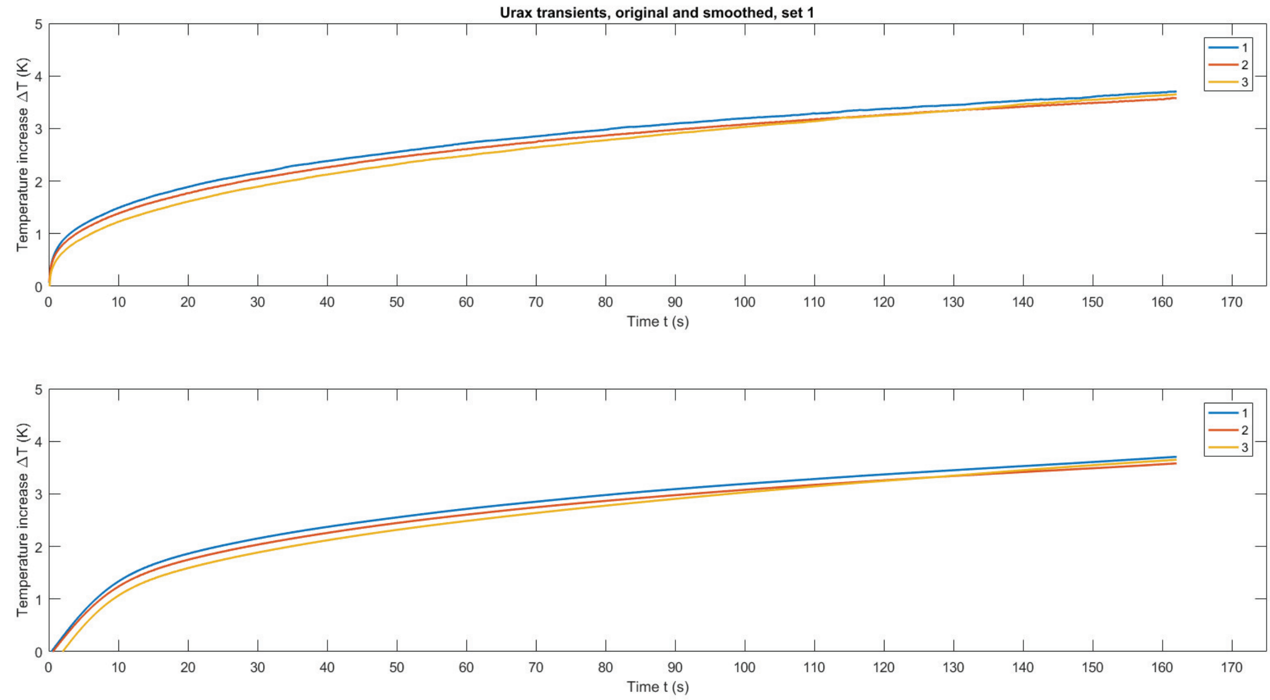

Figure 4.13: Original transient in the top image, smoothed at the bottom.

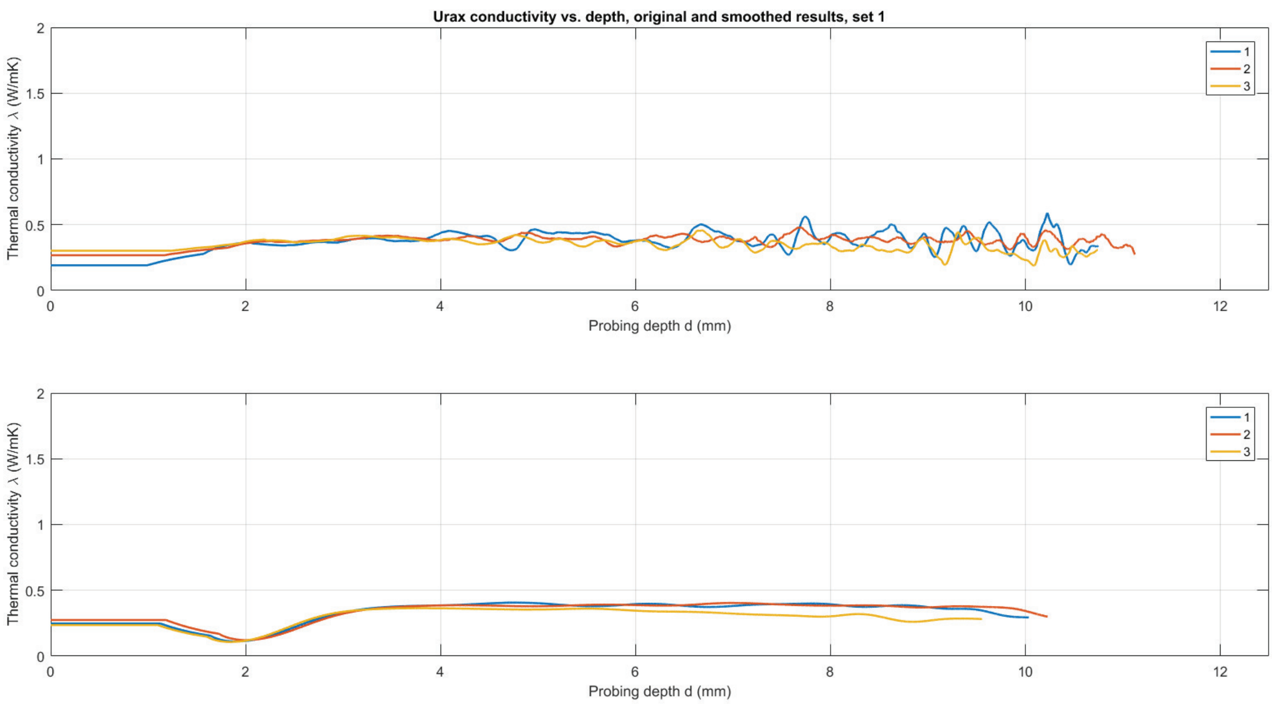

Figure 4.14: Original conductivity vs. depth in the top image, smoothed results in the lower.

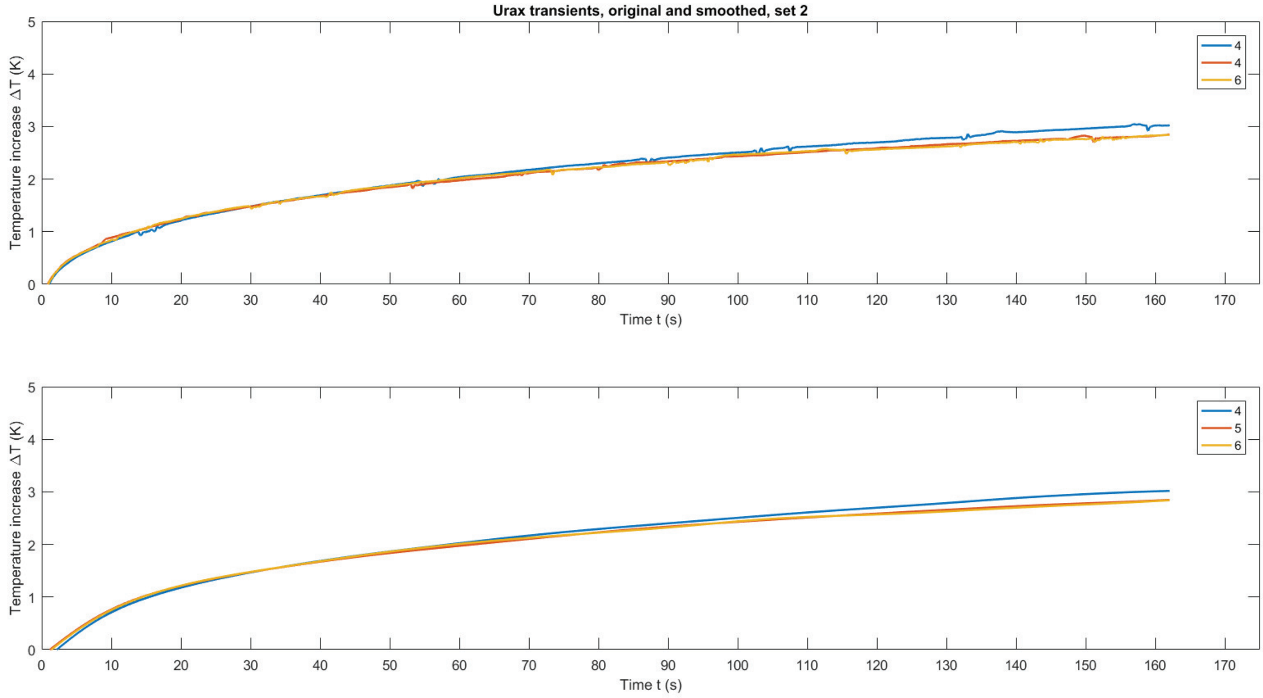

Figure 4.15: Original transient in the top image, smoothed at the bottom.

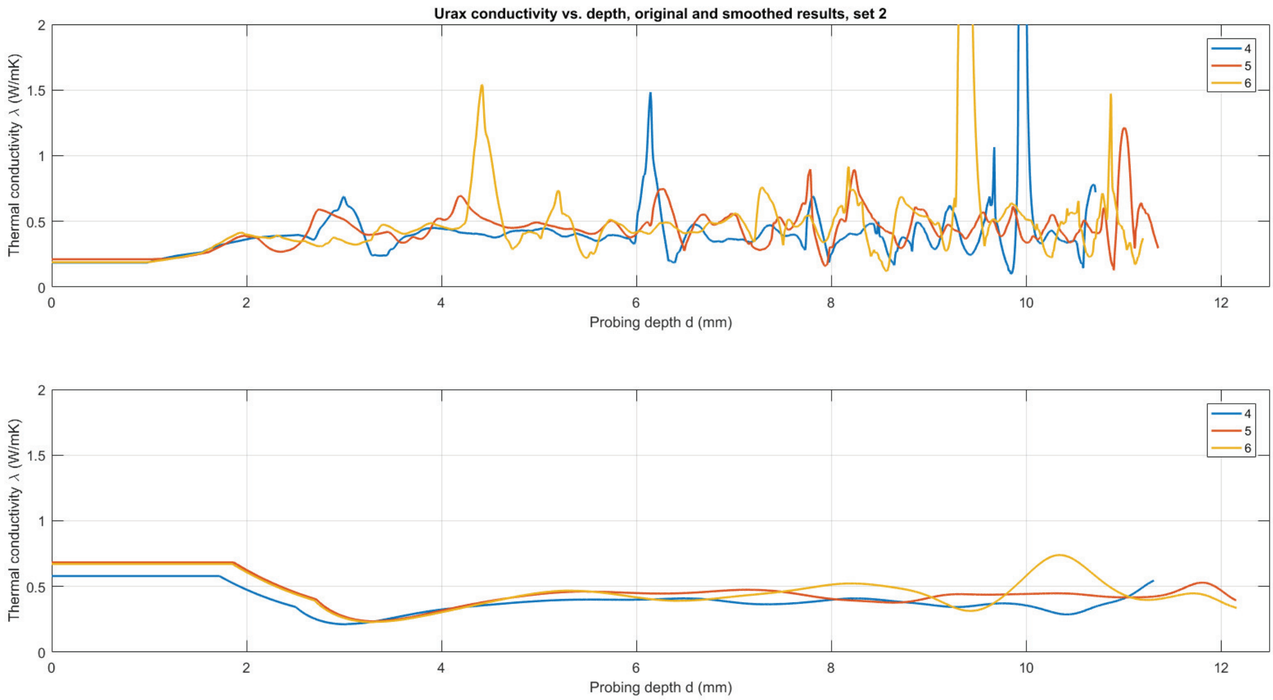

Figure 4.16: Original conductivity vs. depth in the top image, smoothed results in the lower.

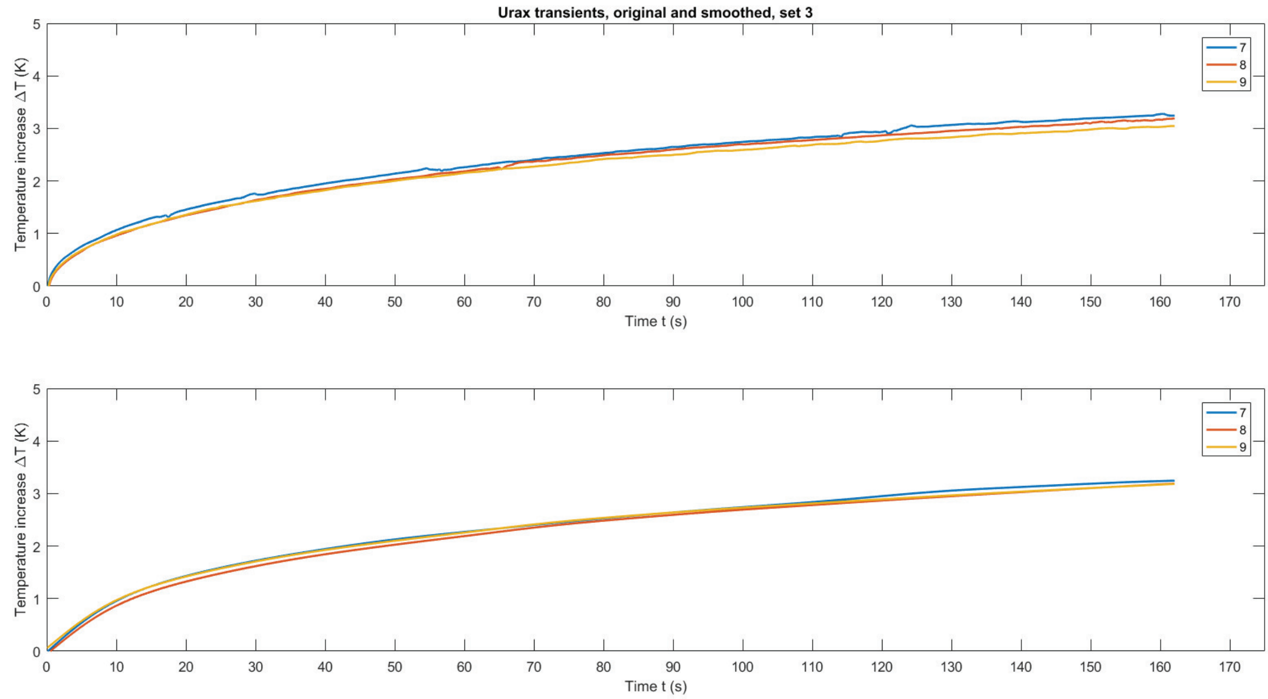

Figure 4.17: Original transient in the top image, smoothed at the bottom.

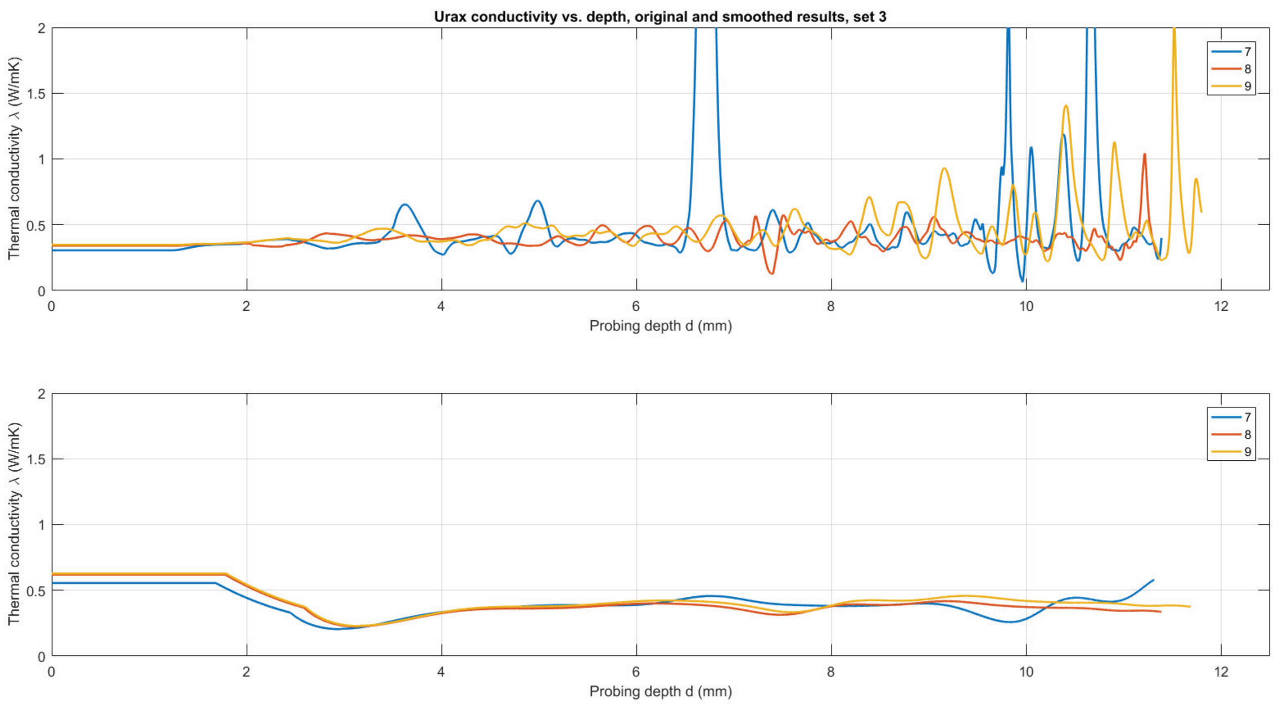

Figure 4.18: Original conductivity vs. depth in the top image, smoothed results in the lower.

4.3 COMSOL Simulation

In figure 4.19, the temperature gradient in the hoof wall resulting from the steady state simulation is shown. It provides the initial conditions for the next step of the simulation where the heat source is switched on. The results from the time dependent simulation is shown in figure 4.20. The total temperature increase in the sensor of 2.83 K was obtained for a heating power of 50 mW.

4.3.1 Conductivity vs. Depth

The transient obtained from the simulation, that is, the temperature development in the heat source, is plotted in figure 4.21. Looking closely, the curve is not as smooth as expected, especially in the first half. This effect is caused by the time steps in the simulation which have been chosen based on the desire to achieve exactly 2000 data points, for easy insertion into the Hot Disk software. In order to avoid the resulting edges affecting the conductivity vs. depth data, the transient is smoothed using the same function in Matlab as the one used for smoothing the live measurement data earlier in this section. The smoothed transient values are then re-calculated into voltages and inserted into the Hot Disk software, such that the program can calculate the conductivity vs. depth curve for the simulated transient for comparison with measurements on live horses.

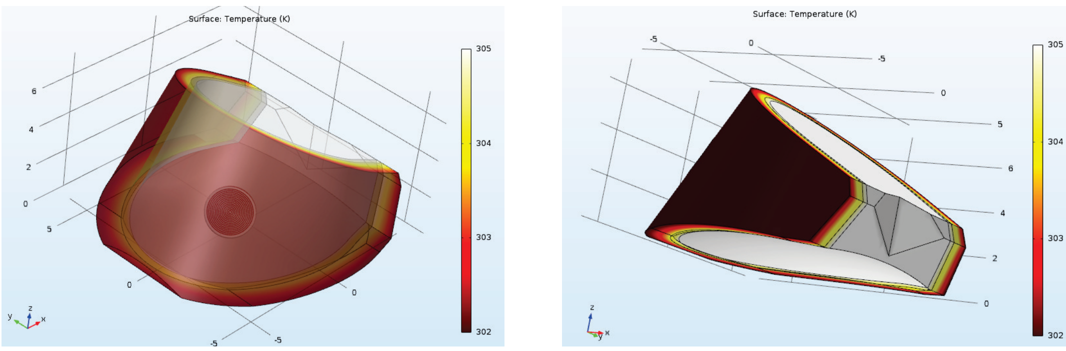

Figure 4.19: Temperature gradient obtained from the steady state simulation.

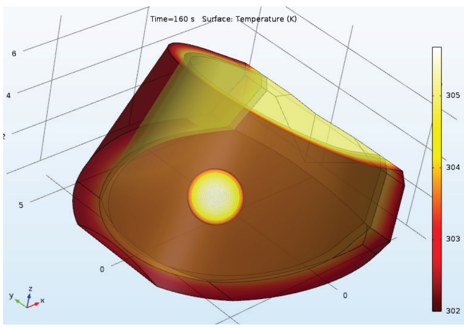

Figure 4.20: Time dependent simulation, sensor heated by 50 mW for 160 s.

The smoothed transient, as well as the calculated conductivity vs. depth curve, are shown in figure 4.22. The thermal conductivity oscillates around 0.4 W/mK, which was the value assigned to the hoof wall in the simulation. At approximately 8 mm depth, the conductivity starts to increase while the oscillations decrease, with values approaching 0.6 W/mK at the end of the curve. The thickness of the hoof wall in the simulation was measured at 7.6 mm, which agrees well with the depth seen in the figure, where the conductivity starts to increase. The next layer is the lamina, with thermal conductivity approximated to that of water at 0.6 W/mK. Comparing this with the live measurements, the same oscillating behavior is seen in all the curves. The increase appearing in the simulation at the hoof wall-lamina boundary could also possibly correspond to a further increasing amplitude in the live measurements at the same approximate depth.

The reason for the oscillations in the simulation is unclear. One thought is that it could have had something to do with the temperature gradient, since it is expected to exist in the live horse hoof as well. However, running the same simulation again without the gradient and instead setting an even initial temperature at 302 K throughout the whole geometry still produced the same oscillating behavior. Therefore, it is possible that it could be caused by the calculation scheme in the software, or the procedure of exchanging values in the Hot Disk files. Furthermore, converting the temperature data from the simulation to voltages is done in a highly approximate way. In fact, this procedure causes the software to believe the voltage values are coming from a real experiment, which they are not. Hence it is unknown how this procedure actually affects the iteration process of the software. Another aspect which matters is that in the simulation, there is perfect thermal contact between the sensor and the hoof. Therefore, the thought behind this part of the study was simply to investigate if the general behavior agreed with what was expected without going into details.

It is, however, interesting to see that it manages do demonstrate the expected conductivity vs. depth of the structure to a certain depth to a satisfying degree.

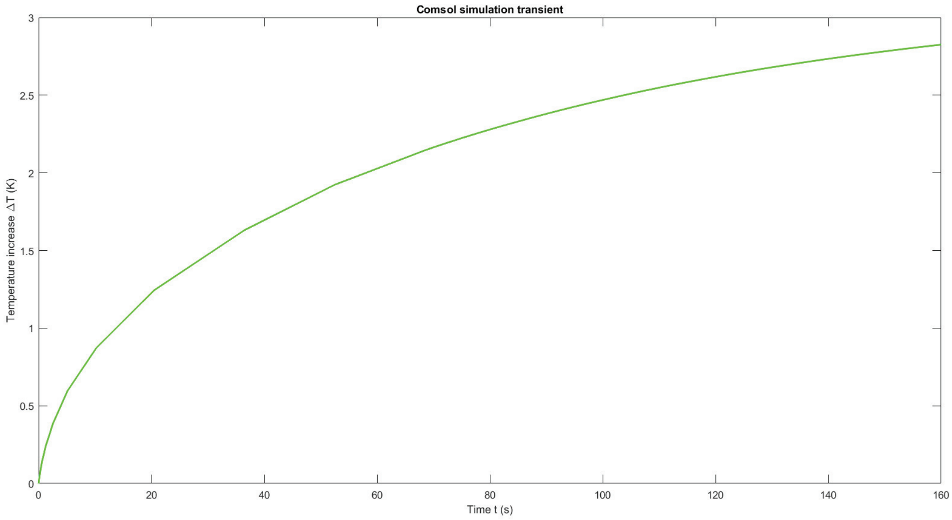

Figure 4.21: Transient obtained in the COMSOL simulation. The first half of the curve is not as smooth as expected, an effect caused by the chosen time step length.

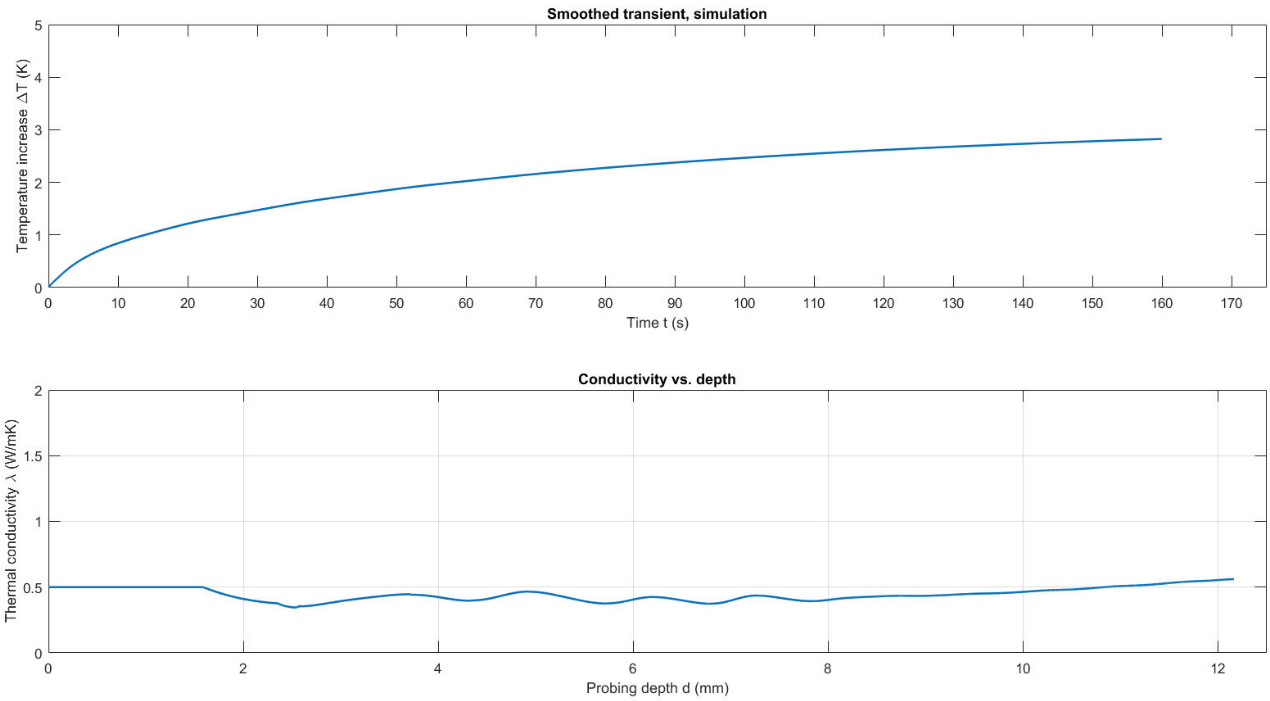

Figure 4.22: The smoothed transient for the simulation is visible in the top image. At the bottom, the corresponding conductivity vs. depth curve is seen.

5

Conclusion

Although more measurement data is recommended, it is indicated in this study that isotropic measurements on both dry and wet hoof wall pieces in the laboratory are reproducible. The average values for conductivity and diffusivity are very similar with very small standard deviations. For live horses, the values are generally higher than for both the dry and soaked hoof piece, and there is also much larger variation in the values obtained. There is no apparent difference between pigmented and unpigmented hooves. Furthermore, the sex and breed of the horse does not seem to affect the values to any significant extent either. Although, more studies are needed before any conclusions are drawn regarding hoof pigmentation, breed and sex of the horse.

There is a rather large variation in the obtained values from live horses, both between individuals as well as different measurements on the same horse. Some of this variation might come from disturbances, for example bad contact between the sensor and the hoof wall. Ensuring good thermal contact is difficult using the current experimental setup on the live horses and therefore, a good prototype which can aid in ensuring even pressure over the sensor without it moving around would be of great help for future study. Another question that needs to be addressed in the near future is whether the measured conductivities will tell us anything about the hoof properties and health status, such as wall strength, wear resistance, localizing damage etc.

For the structural probe measurements, where the conductivity is obtained as a function of probing depth, there are some general features that seem to appear in several of the horses' hooves. Some of these features could possibly be traced to the variation in tubule density across the hoof wall. However, it is sometimes hard to extract any information due to the noise caused by the horse motion. Other factors that are also very likely to affect the measurements are the horses body heat and blood circulation. In previous measurements performed on conserved hooves in a controlled laboratory environment, the structure of the hoof can be relatively clearly distinguished.

When the obtained transient data is smoothed to reduce some of the noise, some key features seem to remain in the conductivity vs. depth curves. Although, the procedure through which this information is obtained is far from optimal. Ideally, a smoothing function would be available in the software which can reduce noise could be of great help if further research is to be carried out on the structural probe measurements. Furthermore, if isotropic measuring, which is a very well established method, produces rather large deviations in accuracy on live horses compared with those of conserved hooves, it would only be fair to expect the accuracy to be worse in the structural probe. The reason for drawing this conclusion is that it is still a new and rather approximate method.

The conductivity vs. depth data calculated from the transient obtained in the simulated experiment in COMSOL multiphysics behave just as expected. The thermal conductivity of the hoof wall region seems approximately correct throughout its thickness, and entering the artificial lamina with properties approximated to those of water indeed shows an increase in thermal conductivity. The conductivity in the hoof wall region displays a wave-like curve similar to the live measurements, although in this case, it is believed to be caused by the not so ideal procedure of inserting values into the software in such a way that the program treats them as if they were coming from a real experiment.

The temperature variation in the hooves, both within the same hoof and between different individuals can be rather dramatic. Within the same hoof, it can either increase, decrease or stay nearly constant during the time of a measurement set, although increase has been the most common. During the experiments, hoof wall temperatures between 11.6 and 32.1°C have been recorded in different horses at different times. Therefore, proper temperature monitoring is important in order to obtain good measurements.

Bibliography

[1] http://www.chalmers.se/en/centres/sportstechnology/research/equestrian-sports/Pages/default.aspx (2017-01-14)

[2] A. N. Hamir, C. Kunz, L. H. Evans, *Equine keratoma*, J Vet Diagn Invest 4:99-100 (1992)

[3] W. Moyer, *Hoof wall defects: cronic hoof wall separations and hoof wall cracks*, Vet Clin Equine 19 463-477 (2003)

[4] P. Ramey *Care and rehabilitation of the equine foot*, Hoof Rehabilitation Publishing, LCC, 2011

[5] K. Hanstorp, B. M. Mihiretie, M. Karlsteen, A. Rosén, M. Sundin, D. Cederkrantz, H. Otterberg, Å. Hinton, B. Berg, *Numerical siumlation and experimental scheme for monitoring hoof wall structure and health in sport horses*, Proceedings of the 4th International Congress on Sport Sciences Research and Technology Support, p. 171-175, (2016)

[6] Y. He, *Rapid thermal conductivity measurement with a hot disk sensor, Part 1. Theoretical considerations,* Thermochimica Acta 436 (2005) 122-129

[7] T. Log, S. E. Gustafsson, *Transient Plane Source (TPS) Technique for Measuring Thermal Transport Properties of Building Materials*, Fire and Materials, vol. 19, 43-49 (1995)

[8] S. E. Gustafsson, *Transient plane source techniques for thermal conductivity and thermal diffusivity measurements of solid materials*, Rev. Sci. Instrum. 62(3), March 1991

[9] B. M. Mihiretie, D. Cederkrantz, M. Sundin, A. Rosén, H. Otterberg, Å. Hinton, B. Berg, M. Karlsteen, *Thermal depth profiling of materials for defect detection using the hot disk technique*, AIP Advances 6, 085217 (2016)

[10] E. Karawacki, B.M. Suleman, *Dynamic plane source technique for simultaneous determination of specific heat, thermal conductivity and thermal diffusivity of metallic samples*, Meas. Sci. Technol. 2 (1991) 744-750

[11] http://www.hotdiskinstruments.com/products/sensors-for-thermal-conductivity-measurements.html (2017-01-15)

[12] A. Sizov, D. Cederkrantz, L. Salmi, A. Rosén, L. Jacobson, S. E. Gustafsson, M, Gustavsson, *Thermal conductivity versus depth profiling of inhomogeneous materials using the hot disc technique*, Rev. Sci. Instrum. 87, 074901 (2016)

[13] http://www.dupont.com/products-and-services/membranes-films/polyimide-films/brands/kapton-polyimide-film.html

[14] H. S. Carslaw, J. C. Jaeger *Conduction of heat in solids*, 2nd ed. Oxford University Press, 1959

[15] *Introduction to heat transfer module*, 1998–2013 COMSOL

[16] https://www.comsol.com/comsol-multiphysics#overview (2017-01-18)

[17] http://www1.agric.gov.ab.ca/$department/deptdocs.nsf/all/4h$7933/file/g_partsofhorse.pdf

[18] C. C. Pollitt, *The anatomy and physiology of the hoof wall*, Equine vet. Educ. (1998) 10 (6) 318-325